Circulation Research

ORIGINAL RESEARCH

Nonbone Marrow CD34+ Cells Are Crucial for Endothelial Repair of Injured Artery

Liujun Jiang,* Ting Chen,* Shasha Sun,* Ruilin Wang, Jiacheng Deng, Lingxia Lyu, Hong Wu, Mei Yang, Xiangyuan Pu, Luping Du, Qishan Chen, Yanhua Hu, Xiaosheng Hu, Yijiang Zhou, Qingbo Xu, Li Zhang

RATIONALE: Endothelial cells play a critical role in multiple cardiovascular diseases. Circulating CD34+ cells are believed to be endothelial progenitors that have been used to treat cardiovascular diseases. However, the exact identity and the role of CD34+ cells in vascular regeneration remains unclear.

OBJECTIVE: We aimed to investigate the exact identity and the role of CD34+ cells in vascular regeneration.

METHODS AND RESULTS: Compared with healthy arteries, CD34 expression percentage was significantly increased in diseased femoral arteries from patients. Using a guidewire-induced endothelial denudation model, we reported the transcriptional profiling of over 30 000 cells by single-cell RNA sequencing analysis and provided a cell atlas of normal and lesioned arteries in mouse, in which a heterogeneous population of CD34+ cells was revealed. Combining the inducible lineage tracing *Cd34*-CreER^{T2};R26-tdTomato mouse model and bone marrow transplantation experiments, we showed that nonbone marrow CD34+ mesenchymal cells acquired endothelial cell fate in the injured femoral artery rather than preexiting endothelial cells, while bone marrow-derived CD34+ cells differentiated into immune cells locally after vessel injury. Depletion of nonbone marrow CD34+ cells using diphtheria toxin-induced cell ablation models exacerbate neointimal lesions of the injured vessel. Furthermore, isolated vascular adventitia CD34+ cells displayed endothelial differentiation, in which microRNA-21-Smad7-pSmad2/3 pathway regulated endothelial gene expression and function during differentiation.

CONCLUSIONS: Our study provides a transcriptional and cellular landscape of vessels after endothelial denudation. Our findings suggest heterogeneous CD34+ cells serve as a contributor not only to endothelial regeneration but also an inflammatory response that may provide therapeutic insights into vascular diseases.

GRAPHIC ABSTRACT: An online graphic abstract is available for this article.

Key Words: CD34 antigens ■ endothelial cells ■ fluorescent antibody technique ■ microRNAs ■ RNA sequence analysis ■ smad proteins ■ vascular system injuries

In This Issue, see p 767 | Meet the First Author, see p 768

Endothelial injury is an initial event in the pathogenesis of vascular diseases, including atherosclerosis, angioplasty-induced vessel injury, and in-stent restenosis.[1] After endothelial damage or denudation in large arteries, regeneration of endothelial cells (ECs) is usually one of the most critical steps in lesion healing. CD34 is a glycophosphoprotein that expressed in hematopoietic stem cells and tissue-resident cells, especially in the vessel wall.[2,3] Concerning bone narrow-derived circulating CD34+ cells, it is well established that they can differentiate into several types of white blood cells. In the late 1990s, Asahara et al[4] isolated CD34+/CD31− cells from peripheral blood and suggested these cells were able to differentiate into ECs in vitro and promote angiogenesis in animal models. These cells were named as endothelial progenitor cells (EPCs). Since then, a large number of studies related to peripheral

Correspondence to: Qingbo Xu, MD, PhD, Department of Cardiology, the First Affiliated Hospital, Zhejiang University School of Medicine, 79 Qingchun Rd, Hangzhou 310003, China, Email qingbo_xu@zju.edu.cn; or Li Zhang, PhD, Department of Cardiology and Institute for Developmental and Regenerative Cardiovascular Medicine, Xinhua Hospital Affiliated to Shanghai Jiaotong University School of Medicine, Shanghai 200092, China, Email li.zhang.uk@gmail.com
*L. Jiang, T. Chen, and S. Sun contributed equally.
The Data Supplement is available with this article at https://www.ahajournals.org/doi/suppl/10.1161/CIRCRESAHA.121.319494.
For Sources of Funding and Disclosures, see page e163.

Circulation Research is available at www.ahajournals.org/journal/res

Novelty and Significance

What Is Known?

- CD34+ cell therapy has been investigated in clinical trials of multiple cardiovascular diseases because these cells might promote angiogenesis or endothelial cell regeneration.
- CD34+ antibody-coated stents fail to achieve ideal clinical benefits in vessel-narrowing diseases.
- Current understanding of the complexity within the CD34+ cell population is not sufficient to explain the problems in translational research of CD34+ cells.

What New Information Does This Article Contribute?

- Our study elucidates the heterogeneity of CD34+ cells at both the single-cell level and the genetically traced level, in the vessel wall of both healthy and wire-injured arteries.
- Nonbone marrow vessel wall CD34+ cells can act as an important source of differentiating and regenerating endothelial cells.
- Specific ablation of nonbone marrow CD34+ cells leads to an aggravation of neointimal formation.
- The microRNA-21-Smad7-pSmad2/3 pathway regulates CD34+ cell differentiation into endothelial cells.

CD34+ cells have been studied for decades as a candidate for stem cell therapy because of their capacity of regenerating endothelial cells and promoting angiogenesis in vitro. However, in most cases, clinical trials using CD34+ cells fail to outperform traditional treatments such as drug-eluting stent implantation, possibly due to the heterogeneity of CD34+ cells and uncontrollable responses in vivo. In this study, we combined single-cell RNA sequencing and genetic lineage tracing to investigate the constitution, distribution, and biological function of vessel wall CD34+ cells and depict the reaction of these cells after wire injury in a mouse model. We revealed that nonbone marrow vessel wall CD34+ cells, which mostly resided in the adventitia, play an important role in regenerating endothelial cells after denudation. Ablation of these cells exacerbated pathological neointimal formation. We also identified the microRNA-21-Smad7-pSmad2/3 pathway by single-cell RNA sequencing and in vitro experiments as a regulator of adventitial CD34+ cells differentiating into endothelial cells. Our study gives a more comprehensive understanding of CD34+ cells.

Nonstandard Abbreviations and Acronyms

BM	bone marrow
BMT	bone marrow transplantation
DTA	diphtheria toxin subunit A
ECs	endothelial cells
EPCs	endothelial progenitor cells
FACS	fluorescence-activated cell sorting
miR-21	microRNA-21
scRNA-seq	single-cell RNA sequencing
SMCs	smooth muscle cells
tdT	tdTomato
TGF	transforming growth factor

blood EPCs have been published, and these CD34+ EPCs have been used as therapeutic agents in hundreds of clinical trials involving ischemia (eg, peripheral arterial disease, coronary artery disease, and myocardial ischemia), pulmonary hypertension, liver cirrhosis, and wound healing.[5–11] Although clinical benefits were achieved in some studies, the outcome of these clinical trials is variable. For example, a previous study has constructed CD34 antibody-coated stents to catch CD34+ cells, which may presumably aid endothelial healing after angioplasty.[12] Although these stents did promote re-endothelialization of the stenting vessel, the side effects of inducing inflammatory responses and exacerbating neointimal formation limited their clinical application.[13] A recent large clinical trial using anti-CD34 antibody-coated combo stent also failed to get a better vascular regeneration.[14] The ambiguous results from studies of EPCs have led to a challenge of the exact identity and function of these EPCs. Recent studies have reported these previously defined EPC populations as circulating monocytes contaminated with platelet microparticles or injured/senescent ECs.[15,16] Thus, whether circulating CD34+ cells in blood are real endothelial progenitors, whether they originated from the bone marrow (BM), and whether they contribute to angiogenesis and participate in vascular repair remain controversial and unresolved for decades.

Meanwhile, reports from several groups have shown the existence of multilineage stem cells in the vessel wall.[17–22] In 2003, Majka et al[23] isolated vascular progenitor cells resident in adult tissues and suggested these cells could be engrafted and differentiated into the endothelium and smooth muscle. Tintut et al[24] also detected stem cell-like cells in the artery wall that demonstrate multipotency in vitro. In 2004, Hu et al[17] provided the first evidence of vascular progenitor cells resident in the adventitia of an adult vessel wall. These adventitial progenitors, characterized by the expression of CD34, Sca-1 (stem cells antigen-1), c-Kit (stem cell factor receptor), and Flk-1 (fetal liver kinase-1), were able to differentiate into smooth muscle cells (SMCs) in vivo and participate in neointima formation.

However, the putative role of these resident CD34+ cells in vascular repair and regeneration in vivo remains elusive.

In this study, we hypothesize that CD34+ cells involved in the vessel wall are a heterogeneous population, in which only a small proportion have a capacity of endothelial regeneration. To test this hypothesis, we first performed single-cell RNA sequencing (scRNA-seq) analysis of mouse femoral artery under physiological condition and in a wire injury-induced endothelial denudation model. We further generated a *Cd34*-CreER^{T2};R26-tdTomato mouse model to label and fate-map endogenous CD34+ cells under both physiological and pathological conditions. Our results demonstrated that CD34+ cells of non-BM origin regenerated ECs in the vessel wall, and further investigate the endothelial differentiation potential of isolated vascular adventitial CD34+ cells in vitro, a process regulated by microRNA-21 (miR-21) via Smad7-pSmad2/3 pathway.

METHODS

Data Availability

The data and R scripts that related to the findings of this study are available on reasonable request. ScRNA-seq data of this study are available in Gene Expression Omnibus (GSE182232). One previously published scRNA-seq data set*28* used in this study is available in the SRA repository (Sequence Read Archive: PRJNA664527).

Detailed description of the studies included and methods used is provided in the Data Supplement. Human sample procedures had local ethical approval. All mice experiments were approved by the Institutional Animal Care and Use Committee of Zhejiang University School of Medicine.

RESULTS

CD34 Expression in Human and Mouse Artery

To detect the expression of CD34 in the blood vessels, we first performed immunostaining in human healthy and diseased arteries (Figure 1A), and in femoral arteries from wild-type mice (Figure I in the Data Supplement). Immunochemistry staining in healthy human internal mammary arteries showed a sporadic distribution of CD34 in the intima and adventitia layer (Figure 1A, upper left). In diseased human femoral arteries with neointima formation, the staining of CD34 was diffusely distributed in the intima layer (Figure 1A, lower left, magnification image 1). In the adventitia layer, newly formed CD34-positive microvessels were observed significantly, which was not detected in healthy artery samples (Figure 1A, lower left, magnification image 2). Statistically, CD34-positive staining varied between groups. The positive staining percentage analysis showed a significantly increased percentage of CD34 expression during artery disease, from 12.85±1.20% in the healthy group to 20.06±1.72% in the diseased group. While the intensity of CD34 staining (calculated by average optical density) was similar between groups (156.58±3.90 in the healthy group and 163.25±6.01 in the disease group), indicating the protein level of CD34 remained unchanged during disease.

The analyses of human arteries revealed an increased number of CD34-expressing cells in artery disease. To further elucidate the underlying cellular mechanism, we performed immunostaining in mouse arteries. CD34 was found to be expressed in both the intimal and adventitial layers of the mouse femoral artery (Figure IA in the Data Supplement). While a minor population of CD34+ ECs was observed in both the intima and adventitia, a large group of CD34+CD31− cells were detected in the adventitial layer, indicating vascular CD34+ cells as a heterogeneous population. Apart from the arterial wall, BM is also a classic and established source for CD34+ cells. Notably, CD34+ BM cells were partially copositive for other progenitor cell markers such as Sca-1 or c-Kit (Figure IB in the Data Supplement).

Single-Cell Transcriptomes of CD34+ Cells in the Mouse Femoral Artery

To delineate the exact nature and cellular heterogeneity of CD34+ cells in mouse vessels, single nucleated live cells (Hoechst+/dead cell stain−) were isolated from the whole femoral arteries of 10- to 12-week-old wild-type C57BL/6J mice by enzymatic digestion (Figure IIA in the Data Supplement). Both male and female mice were included to acquire an unbiased result. Cells were then processed for scRNA-seq using the 10× Chromium platform (Figure IIB in the Data Supplement). A total of 5170 cells passed quality control metrics and were further analyzed. At a sequencing depth of 30 mol/L per cell, 2310 genes were detected per cell on average (Table II in the Data Supplement). Using Seurat,[25] unsupervised clustering with t-distributed stochastic neighbor embedding analysis revealed 15 cell clusters, which were further attributed to putative biological identities based on differentially expressed signature genes (Figure 1B, Figure IIC and Table III in the Data Supplement). The cell clusters comprised vascular SMCs (3 clusters; *Myh11*, *Cnn1*, *Acta2*, *Tagln*), ECs (2 clusters; *Pecam1*, *Vwf*, *Cdh5*), mesenchymal cells (5 clusters; *Sfrp2*, *Comp*, *Igfbp6*), B cells (*Cd79a*, *Cd79b*), T cells (*Cd3d*, *Csf2*), monocytes/macrophages (*Cd14*, *Ccl4*), and pericytes (2 clusters; *Mcam*, *Actg2*, Figure IID in the Data Supplement). Of note, CD34 was expressed in a large population of mesenchymal cells and ECs of arteries (Figure 1C). Previously reported progenitor cell markers, such as *Mcam*, *Kdr*, *Klf*4, and *Kit*, were also examined in femoral artery cells (Figure IID in the Data Supplement). We found that *Klf4* was highly expressed in mesenchymal and endothelial populations. The endothelial clusters also expressed *Kdr*, while most SMC clusters express CD146 (*Mcam*). However, *Kit* was rarely detected in our scRNA-seq data.

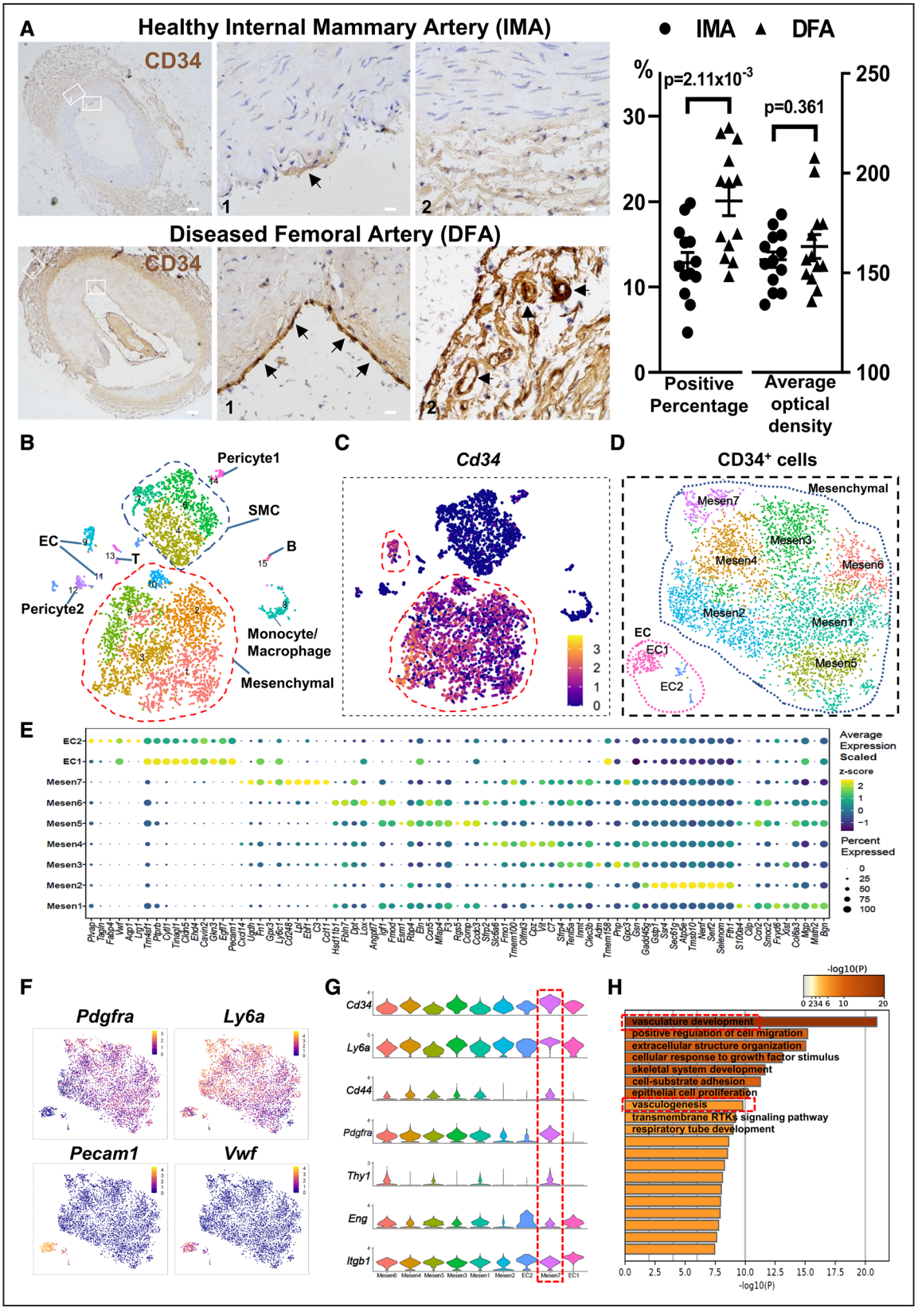

Figure 1. Single-cell RNA sequencing (scRNA-seq) analyses of CD34+ cells in femoral artery cells.
A, Representative images of CD34 expression in human internal mammary artery (IMA) and diseased femoral artery (DFA), with magnification of the boxed region. Arrows indicate positive staining cells. Scale bars: 200 μm and 20 μm in magnification images. Dot plot (**right**) showed the percentage and average optical density of CD34 positive staining across different groups (n=13 in each group). Data represent mean±SEM. Data were first tested and passed normality test (D'Agostino and Pearson test), and unpaired 2-tailed *t* tests (*Continued*)

We further sought to investigate the heterogeneity of CD34+ cells from the single-cell level. An additional digestion of C57BL6/J mouse femoral arteries was performed, CD34+ cells were specifically isolated by fluorescence-activated cell sorting (FACS) using anti-CD34 antibody and subjected for scRNA-seq. A total of 6668 cells were acquired by FACS sorting and scRNA-seq data analysis for selecting cells expressing *Cd34* gene (Figure 1D). We also compare FACS based protein CD34+ cells and gene *Cd34*+ cells which were selected from the original scRNA-seq data set. Interestingly, protein CD34 were only expressed on large amount of mesenchymal cell and a minor population of ECs (Figure 1D and Figure IIIA in the Data Supplement), while gene *Cd34* also weakly distributed on SMCs and less macrophages (Figure IIIA in the Data Supplement). Further analyses of CD34+ cells were based on the FACS sorted protein CD34+ cell data set. CD34+ cell populations were further clustered as 9 subpopulations (or 2 main groups), characterized by distinct marker genes (Figure 1E and 1F and Figure IIIB and Table IV in the Data Supplement). Endothelial marker genes *Pecam1* and *Vwf* were restricted in the 2 EC populations, while mesenchymal marker *Pdgfra* was only seen in mesenchymal populations. Interestingly, previously reported progenitor maker *Ly6a* (encoding stem cell antigen-1, Sca-1) was highly expressed in both mesenchymal and ECs. Progenitor marker *Kit*, however, was rarely expressed across cells. The most abundant CD34+ cell population detected was mesenchymal cells, including 7 subclusters. Interestingly, we characterized a distinct population (mesenchymal cell 7) highly expressing progenitor markers, including *Cd34*, *Ly6a*, *Pdgfra*, and *Thy1* (Figure 1G). Gene enrichment analysis for hallmark pathways in mesenchymal cell 7 revealed enriched terms including vasculature development and vasculogenesis (Figure 1H), indicating a progenitor phenomenon. In the EC populations, we also compared protein CD34+ cells and gene *Cd34*- cells from the original femoral artery data set. Differential gene analysis showed multiple differentially expressed genes between 2 EC subtypes, while protein CD34+ EC acquired a stronger capacity of endothelium development and blood vessel morphogenesis (Figure IIIC in the Data Supplement). Collectively, our data provided a single-cell atlas of mouse femoral artery and further suggested a heterogeneous CD34+ cell population, including cells in a subpopulation exhibited high angiogenic potential.

Lineage Tracing Study Showing Distribution of CD34+ Cells in Mouse Femoral Artery

To further confirm the heterogeneity of CD34+ cells and reveal the nature and location of endogenous CD34-expressing and derived cells in the mouse femoral artery of adult mice (8 weeks old at the start of each experiment), we designed a CreER^{T2} knockin strategy within the *Cd34* gene locus and generated a novel *Cd34*-CreER^{T2} mouse line. We then conducted an inducible genetic lineage tracing system for CD34+ cells by crossing *Cd34*-CreER^{T2} with R26-tdTomato mouse lines (Figure IVA in the Data Supplement). The *Cd34*-CreER^{T2};R26-tdTomato mice were treated with 4 intermittent pulses of tamoxifen to induce tdTomato labeling of CD34+ cells, and tissue was collected for analysis 1 week later (Figure IVB in the Data Supplement). To test the labeling effect of CD34, we first detected tdTomato and CD34 expression in major organs. Coexpression of CD34 and tdTomato was widely observed in the heart, lung, liver, kidney, spleen, and aorta (Figure IVC in the Data Supplement). These data demonstrated that the tdTomato signal faithfully represented CD34+ cells.

We then focused on the femoral artery and could readily detect tdTomato fluorescence in the whole-mount artery samples after tamoxifen treatment (Figure VA in the Data Supplement). Immunostaining for tdTomato and CD34 showed strong colocalization, either on dissociated cells from arteries or on artery sections (Figure 2A), with over 90% of tdTomato+ cells expressing CD34. Of note, most CD34+ cells reside in the adventitia of the femoral artery and could hardly be seen in the intima. Flow cytometric analyses of dissociated femoral artery cells (Figure 2B) showed that 97% tdTomato+ cells coexpressed CD34, and 61% of CD34+ cells were labeled with tdTomato, indicating a high specificity and efficiency of *Cd34*-CreER for lineage tracing of CD34+ cells in the femoral artery. To further identify the cell types labeled by CD34 in the vessel, we sectioned femoral arteries for immunostaining of tdTomato and possible cell lineage markers. Results showed that only 3% to 4% of tdTomato+ cells coexpressed EC markers CD31 or CD144 (Figure 2C and 2D), which was also confirmed by flow cytometric analyses. Immunostaining and flow cytometric analysis of hematopoietic marker CD45 also indicated the presence of CD34+ CD45+ leucocyte population (1%–3%, Figure 2E). In the adventitial layers, where most CD34+ cells were located, we observed

Figure 1. Continued (with homogeneity of variances tested) were performed. *P* values of each comparison were specified in the graph, $P<0.05$ was considered to be statistically significant. **B**, Visualization of unsupervised clustering in a t-distributed stochastic neighbor embedding (t-SNE) plot of 5170 cells isolated from normal C57BL6/J mice femoral arteries. **C**, Feature plot showing expression of CD34 across all populations. **D**, T-SNE plot of the fluorescence-activated cell sorting (FACS) sorted CD34+ cells. n=6668 cells. **E**, Dot plot showing average scaled expression levels (color-scaled, column-wise *Z* scores) of top differentially expressed genes (DEGs; columns) across the CD34+ cell subpopulations (rows), cells with a value >0 represent cells with expression above the population mean. Dot size reflects the percentage of cells expressing the selected gene in each population. **F**, Feature plot showing expression of gene markers of SPC (*Pdgfra* and *Ly6a*) and endothelial cell (EC; *Pecam1* and *Vwf*) across all populations. **G**, Violin plots showing the expression levels of progenitor markers across the CD34+ cell subpopulations. Mesenchymal cell (Mesen) 7 with higher expression of progenitor markers was marked in dashed box. **H**, Top 10 hallmark pathways enriched in Mesen 7 cluster.

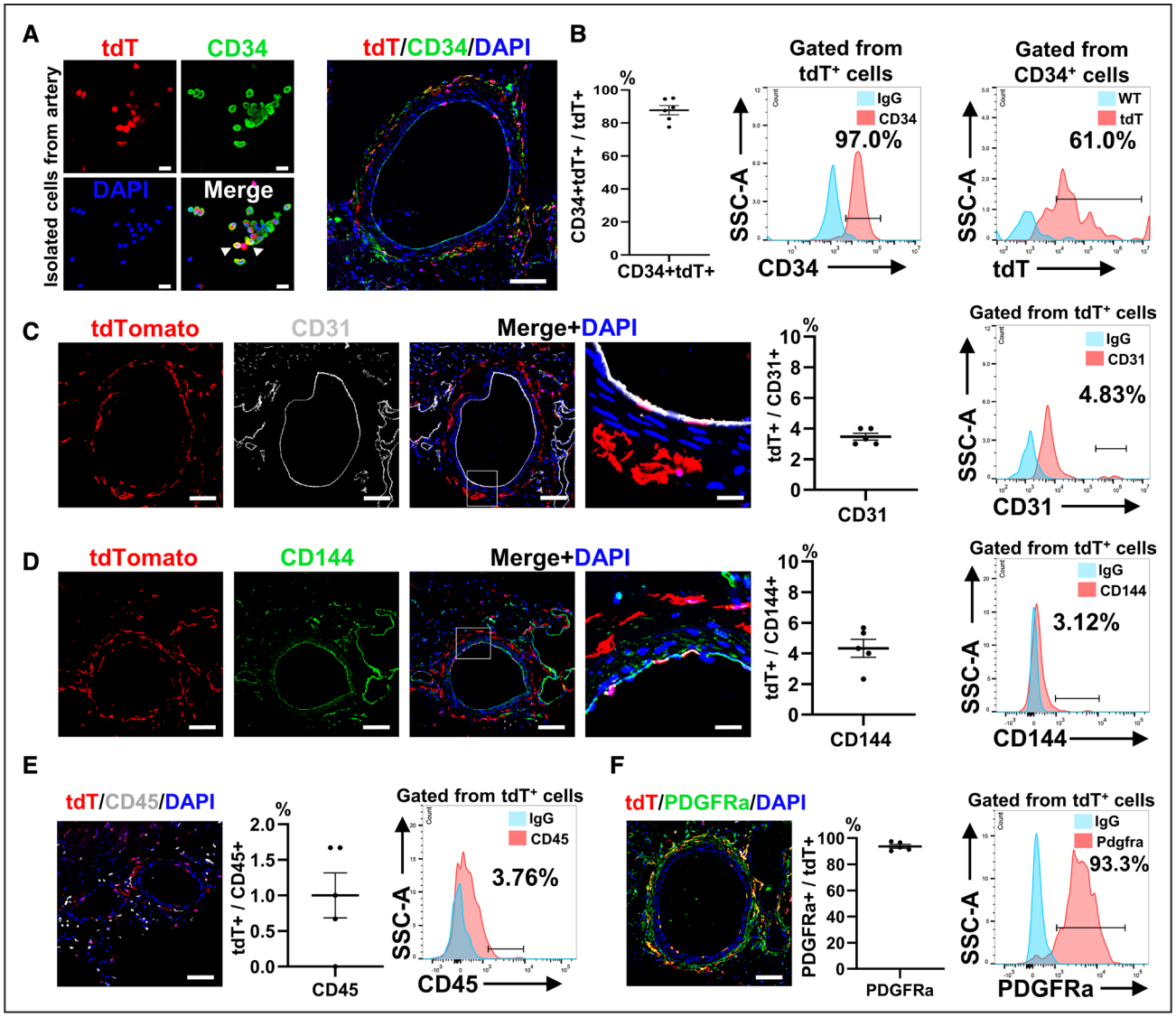

Figure 2. Characterization of CD34⁺ cells in mouse femoral artery.
A, Immunostaining for tdTomato (tdT) and CD34 on isolated cells from arteries and on femoral artery sections, with quantification of the percentage of CD34⁺ cells in tdT⁺ cells. **B**, Flow cytometric quantification of the percentage of CD34⁺ cells in tdT⁺ cells (**left**) and tdT expression in CD34⁺ cells (**right**). **C**, Immunostaining for tdT and CD31 on a femoral artery section with magnification of the boxed region. Fluorescent and flow cytometric quantification of the labeled CD31⁺ cells by *Cd34*-CreER^{T2} were displayed on the **right**. **D**, Immunostaining for tdT and CD144 on a femoral artery section with magnification of the boxed region. Fluorescent and flow cytometric quantification of the labeled CD144⁺ cells in tdT⁺ cells were displayed on the **right**. **E**, Immunostaining for tdT and CD45 on a femoral artery section, with fluorescent and flow cytometric quantification of CD45⁺ cells in tdT⁺ cells. **F**, Immunostaining for tdT and PDGFRa (platelet-derived growth factor receptor A) on a femoral artery, with fluorescent and flow cytometric quantification of PDGFRa⁺ cells in tdT⁺ cells. Scale bars, 100 μm and 20 μm in magnification images. Data are mean±SEM, n=6 in (**A**) and n=5 in **C–F**). Cell sample in each flow cytometric analysis were pooled cells of dissolved femoral arteries from 6 *Cd34*-CreER^{T2};R26-tdT mice after tamoxifen treatment.

that over 90% tdTomato⁺ cells expressed PDGFRa (platelet-derived growth factor receptor A), indicating that these cells as mesenchymal cells (Figures 2F). These above data were consistent with our above scRNA-seq analyses, showing CD34⁺ cells as possible mesenchymal cells, ECs, and leucocytes. Furthermore, we did not detect any tdTomato⁺ fluorescence in SMCs in the media layer (Figure VB in the Data Supplement). Additional staining also excluded CD34⁺ cells as perilipin A⁺ (PLIN⁺) adipocytes around the artery (Figure VC in the Data Supplement). Taken together, we showed that in the artery wall, CD34⁺ cells are a heterogeneous population, including a significant proportion of adventitial mesenchymal cells, a tiny population of ECs and leucocytes, but not medial SMCs.

Nonmature EC Source of CD34⁺ Cells Regenerate Endothelium After Denudation

We next evaluated how CD34⁺ cells were involved in vascular remodeling under diseased condition. We examined

whether CD34+ cells divide them into new cells during homeostasis or after vascular injury. Mouse femoral arteries were collected 12 weeks after tamoxifen treatment (Figure VIA in the Data Supplement). Immunostaining and quantification for tdTomato and CD34 revealed that under homeostasis condition CD34+ cells remained a low percentage without self-expansion (Figure VIB in the Data Supplement). Femoral artery guidewire injury surgery was performed to denudate the endothelium, then injured artery samples were collected at different stages: the early endothelial repair stage (day 1 to day 14) for en-face staining and later stage (2 and 4 weeks after injury) for cross sections (Figures VIIA and IXA in the Data Supplement). Strong tdTomato fluorescence in the whole-mount postinjury artery sample was observed (Figure IXB in the Data Supplement). For early stage analyses, we also used *Cdh5*-CreER^{T2};R26-tdTomato mice (mature EC lineage tracing model) to evaluate the contribution of preexisting mature EC in this injury model. Injured arteries were separated into 2 parts: the centric injured region and the adjacent regions (Figure VIIB in the Data Supplement). Surprisingly, different repair patterns were observed in these 2 regions. The ECs in the centric region were regenerated more from CD34+ cells rather than mature *Cdh5*-lineage ECs (Figure 3A and 3B). While ECs in the adjacent region were mostly repaired by mature ECs, while CD34+ cells also contribute to the process (Figure VIIC and VIID in the Data Supplement). For later stage analyses, sections from artery tissue at the same time points were stained for tdTomato and a collection of lineage markers. Unlike the distribution of CD34+ cells in physiological arteries (Figure 3C), which tdTomato+ CD31+ cells only accounted for a minor population of ECs, a large number of tdTomato+ CD31+ ECs were observed in the intimal layer in diseased condition (Figure 3D), with a growing trend over time. Quantitatively, an increased number of tdTomato+ ECs could be observed over time, from 6.34±2.61% in the sham group, to 29.09±3.29% in the 2-week group, and finally to 44.84±7.66% in the 4-week group (Figure 3E). This was further confirmed by flow cytometric analysis, showing that over half of the CD31+ dissociated vessel cells coexpressed tdTomato (Figure 3F).

Except for the luminal ECs, there was also adventitia microvessel expansion after vascular injury. To investigate CD34+ cell's contribution on this process, we performed tissue clearing and 3-dimensional imaging to display a full picture of the outer layer. Compared with normal arteries, abundant newly expanded microvessels were observed in the adventitia, costained with CD34-lineage marker tdTomato, indicating a major contribution of CD34+ cells in the adventitia microvessel formation (Figure VIIIA through VIIIC in the Data Supplement). Verification on tissue sections also confirmed these results (Figure VIIID in the Data Supplement). Similar findings were observed with CD144 staining, as well as additional Vcam-1 (vascular cell adhesion molecule 1) and eNOS (endothelial nitric oxide synthase) staining (Figure XA through XC in the Data Supplement), with similar statistical results that CD34+-derived tdTomato+ ECs contributed about half of newly expanded ECs after vascular injury (Figure XD and XE in the Data Supplement). Interestingly, newly regenerated ECs from later stage analysis did not express CD34, suggesting CD34 as an early phase cell marker in diseased condition (Figure XIA in the Data Supplement). These data collectively suggest that CD34+ cells contribute to both luminal endothelial regeneration and microvessel remodeling in the injured artery.

Consistent with the observation from the normal femoral artery (Figure VB in the Data Supplement), immunostaining of injured vessels showed that the vessel wall was devoid of tdTomato+ SMCs after wire injury, neither in the native media layer nor in the neointima (Figure IXC and IXD in the Data Supplement). Considering that inflammation plays a pivotal role in vascular injury,[26,27] we also examined the potential role of CD34+ cells in inflammation in this model. Immunostaining for tdTomato and hematopoietic marker CD45 showed a contribution of CD34+ cells to CD45+ inflammatory cells and especially CD11b+ macrophages (Figure IXE in the Data Supplement). Statistical analysis of immunostaining and flow cytometric analysis revealed that 50% to 60% of CD45+ cells were positive for tdTomato (Figure IXF and IXG in the Data Supplement), suggesting a considerable number of CD34+ cells participate in the local inflammatory response. Lesional leukocytes also did not express CD34 in the later stage of disease (Figure XIB in the Data Supplement).

Additionally, we compared our C57BL6/J mouse femoral artery scRNA-seq data set with a published mouse aorta data set[28] to find the difference between these 2 vessels. The cell component differed largely between aortic and femoral arterial cells, as aorta comprised large populations of lymphocytes, and cell component of SMCs and ECs also differed from each other. The 4 SMC subtypes and 2 EC subtypes exhibited different distribution in 2 types of vessels, indicating different pathophysiological roles of vascular cells in different vessels (Figure XIIA and XIIB in the Data Supplement). Further analyses using multiple differentially expressed genes and gene ontology (GO) methods indicated that femoral ECs displayed lower abilities for EC differentiation and cell migration (Figure XIIC and XIID in the Data Supplement), which suggested some additional regenerating sources such as CD34+ cells in our above analyses.

Non-BM Source of CD34+ Cells Contribute to Endothelial Regeneration While BM CD34+ Cells Give Rise to CD45+ Leucocytes During Neointimal Formation

Our above data revealed abundant CD34+ cells in the vascular injury model. We next sought to address whether these CD34+ cells originate from BM or non-BM source.

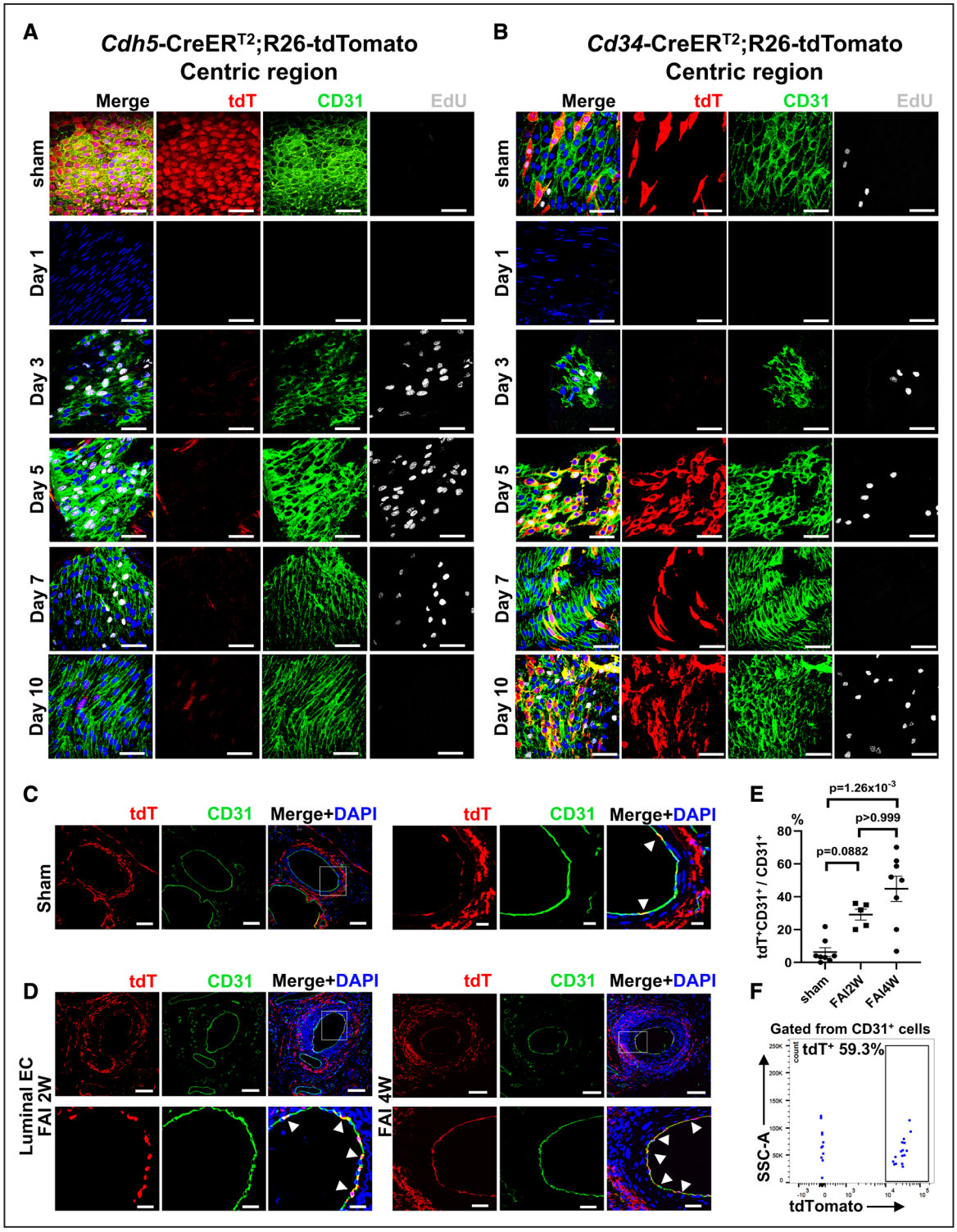

Figure 3. Nonmature endothelial cell (EC) source of CD34⁺ cells repopulate ECs in neointima formation.
A, En-face immunostaining for tdTomato (tdT), CD31, and proliferation marker EdU on the centric intimal layer of *Cdh5*-CreER^{T2};R26-tdT mice at indicated time point. Scale bars, 50 μm. **B**, En-face immunostaining for tdT, CD31 and proliferation marker EdU (5-Ethynyl-2'-deoxyuridine) on the centric intimal layer of *Cd34*-CreER^{T2};R26-tdT mice at indicated time point. Scale bars, 50 μm. **C**, Immunostaining for tdT and CD31 on femoral artery sections from the sham group, with magnification of the boxed region. **D**, Immunostaining for tdT and CD31 on femoral artery sections from the femoral artery injury (FAI)-2 wk (FAI2W) group (**left**) and the FAI-4 wk (FAI4W) group (**right**) relating to luminal ECs, with magnification of the boxed region. **E**, Quantification of the percentage of CD31⁺ tdT⁺ cells in CD31⁺ cells at different time points. Scale bars, 100 μm and 20 μm in magnification. Data represent mean±SEM, n=8 in the sham and FAI4W groups and n=5 in the FAI2W group. Data were first tested by Shapiro-Wilk test for normality and nonparametric 1-way ANNOVA test (Kruskal-Wallis test with Dunn multiple comparisons test) was performed. *P* values between each 2 groups were specified in the graph, $P<0.05$ was considered to be statistically significant. **F**, Flow cytometric analysis of CD31 expression in tdT⁺ cells. Cells used in the flow cytometric analysis were pooled cells of dissolved femoral arteries from 6 *Cd34*-CreER^{T2};R26-tdT mice at FAI4W group.

Using a BM transplantation (BMT) model, 2 types of chimeric mice were generated: one in which BM cells from *Cd34*-CreER^{T2};R26-tdTomato mice were transferred to irradiated wild-type C57BL/6J mice (BMT$^{CD34\rightarrow WT}$), and another vice versa (BMT$^{WT\rightarrow CD34}$). The chimeric mice were then pulsed with tamoxifen and subjected to femoral artery injury or euthanized for reconstitution analyses (Figure 4A). Successful reconstitution of BM in BMT$^{CD34\rightarrow WT}$ chimeric mouse was confirmed by the detection of tdTomato$^+$ cells in BM by flow cytometry and on isolated cells by immunostaining 1 week after tamoxifen usage (Figure XIIIA in the Data Supplement). The reserve

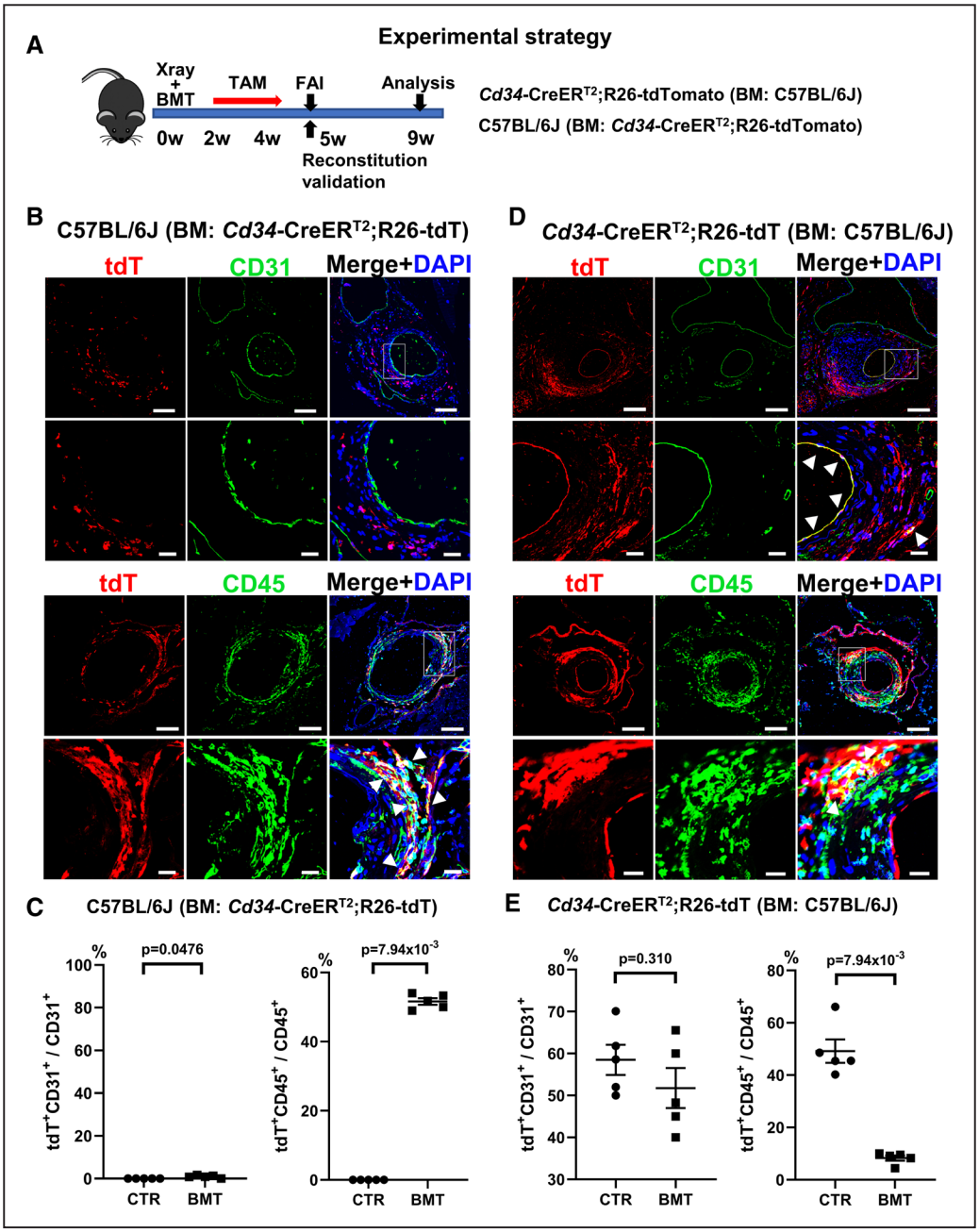

Figure 4. Nonbone marrow CD34$^+$ cells repopulate endothelial cells, whereas bone marrow (BM) CD34$^+$ cells give rise to CD45$^+$ leukocytes in neointima formation.

A, Sketch of the experimental design for BM transplantation (BMT) to generate 2 types of chimeric mice. **B** and **D**, Immunostaining for tdTomato (tdT), CD31 and CD45 on wire-injured femoral artery sections from 2 types of chimeric mice. **C** and **E**, Quantification of the percentage of tdT expression in CD31$^+$ or CD45$^+$ cells from injured femoral arteries of 2 types of chimeric mice. C57BL/6J mice (**C**) or *Cd34*-CreER^{T2};R26-tdT mice (**E**) without BMT were used as controls (CTR). Arrow heads indicate coexpressing cells. Scale bars, 100 μm and 20 μm in magnification. Data represent mean±SEM, n=5 in each group. Data were tested by unpaired nonparametric 2-tailed Mann-Whitney *U* test. *P* values between each 2 groups were specified in the graph, $P<0.05$ was considered to be statistically significant. FAI indicates femoral artery injury.

of CD34+ cells before and after BMT revealed they were radioresistant (Figure XIIIC and XIIID in the Data Supplement). In this chimeric mouse model ($BMT^{CD34\rightarrow WT}$), tdTomato+ cells were detected mainly in the adventitial layers of the postinjury artery sections. Coexpressing of tdTomato in CD31+ ECs were rarely observed neither on the luminal surface nor in the adventitia (Figure 4B and 4C). However, we observed a large number of tdTomato+ CD45+ cells in the $BMT^{CD34\rightarrow WT}$ chimeric mouse (Figure 4B), with 51.62±0.95% of CD45+ cells positive for tdTomato (Figure 4C). It should be noted that a number of tdTomato− CD45+ cells were also observed in this chimeric model. Conversely, in another $BMT^{WT\rightarrow CD34}$ chimeric mouse model, which manifested nearly complete abolishment of tdTomato+ cells in the BM (Figure XIIIB in the Data Supplement), a small number (8.29±1.01%) of tdTomato+ CD45+ cells were also observed, indicating that CD34+ cells from a non-BM origin, such as the vessel wall or adjacent tissues, also contribute to the inflammatory response, although accounting for a small population (Figure 4E). In addition, coexpression of tdTomato in CD31+ ECs was frequently observed on the luminal surface and in the adventitia (Figure 4D), with an average percentage similar to that in non-BM *Cd34*-$CreER^{T2}$;R26-tdTomato mice (51.78±4.76% in BMT group compared with 58.51±3.61% in the control group, Figure 4E). Traditionally, BM or circulating EPCs were thought to be the major source of ECs postvascular injury. However, our above data critically demonstrated that most luminal and microvessel CD31+ ECs are derived from non-BM CD34+ cells in response to vascular injury, while BM CD34+ cells mainly give rise to increased CD45+ leucocytes, which may also be an important contributor to neointima formation.

Depletion of Non-BM CD34+ Cells Aggravates Neointimal Lesions

Our data so far suggested that non-BM CD34+ cells regenerated ECs while BM CD34+ cells generate leucocytes. We next sought to address the functional role of CD34+ cells in vessel repair and regeneration. To test the possible function of CD34+-derived cells, we crossed the *Cd34*-$CreER^{T2}$;R26-tdTomato and R26-eGFP-diphtheria toxin subunit A (DTA) mouse lines to allow selective ablation of the CD34+ cell population at indicated time points. Cre recombinase activation by tamoxifen administration leads to the specific expression and activation of the DTA in CD34+ cells, resulting in termination of protein synthesis and apoptotic cell death.[29] We treated the mice with tamoxifen before and after vessel injury with 2 full-dose pulses to achieve a thorough depletion of CD34+ cells during the perioperative period (Figure 5A). *Cd34*-$CreER^{T2}$;R26-tdTomato mice were used as control. After tamoxifen induction on *Cd34*-$CreER^{T2}$;R26-DTA/tdTomato mice, 60% to 70% of CD34+ cells were depleted in the vessel wall and the BM as verified by flow cytometric analyses (Figure 5B and Figure XIVA in the Data Supplement), along with a significant decrease of tdTomato fluorescence in whole-mount samples (Figure 5C). As DTA targeting all CD34-expressing cells, by flow cytometry we detected a decrease of tdTomato+ CD31+ ECs (Figure XIVB in the Data Supplement, left compared with Figure 2C) and tdTomato+ PDGFRa+ mesenchymal cells (Figure XIVB in the Data Supplement, right compared with Figure 2F). After vessel injury, histological examination showed an increase in lumen area, with decrease in neointima thickness and neointima/media ratio (Figure 5D and 5E). Immunostaining for tdTomato and cell lineage markers further showed a significant decrease of tdTomato+ CD31+ or tdTomato+ CD144+ ECs (Figure 5F and 5G), leucocytes (Figure XIVC in the Data Supplement) and mesenchymal cells (Figure XIVD in the Data Supplement).

Since our above data indicated a non-BM source of CD34+ cells regenerating ECs, to address the exact role of the non-BM CD34+ cells, we created a selectively non-BM CD34+ cell ablating model, that chimeric mice were generated by transferring C57BL/6J BM cells into irradiated *Cd34*-$CreER^{T2}$;R26-DTA/tdTomato mice (Figure XIVE in the Data Supplement). After tamoxifen administration and vessel injury (Figure 5H), we observed a notable aggravation of neointima formation in the chimeric DTA group with decreased lumen area, increased neointima thickness and intima/media ratio (Figure 5I and 5J). Immunostaining analyses exhibited a similar decrease of tdTomato+ CD31+ or tdTomato+ CD144+ ECs (Figure 5K and 5L) and mesenchymal cells (Figure XIVG in the Data Supplement). Since wild-type BM cells were transferred, the BM-originated CD34+ cells were not affected by DTA, as evidenced by CD45+ cells remained in artery sections (Figure XIVF in the Data Supplement).

By using *Cd34*-$CreER^{T2}$;R26-DTA/tdTomato mice, we gave tamoxifen both to label CD34-lineage cells and also to specifically ablate them. We also crossed *Cd34*-$CreER^{T2}$;R26-tdTomato mice with R26-DTR mice to obtain *Cd34*-$CreER^{T2}$;R26-DTR/tdTomato mice. Tamoxifen was only used for labeling cells and exogenous diphtheria toxin injection was used for depleting cells thereafter. Similar findings were also verified in this mouse model (Figure XV in the Data Supplement). Taken together, our data support that in the wire injury model, different origins of CD34+ cells possess different pathological contributions, that BM CD34+ cells were pathogenic factors by their inflammatory components while non-BM CD34+ cells were protective factors via their endothelial and mesenchymal functions.

Single-Cell Transcriptomes Depict Cellular Landscape in Vascular Injury

To depict the cellular changes (including tdTomato-labeled CD34+ cells) and examine possible mechanisms

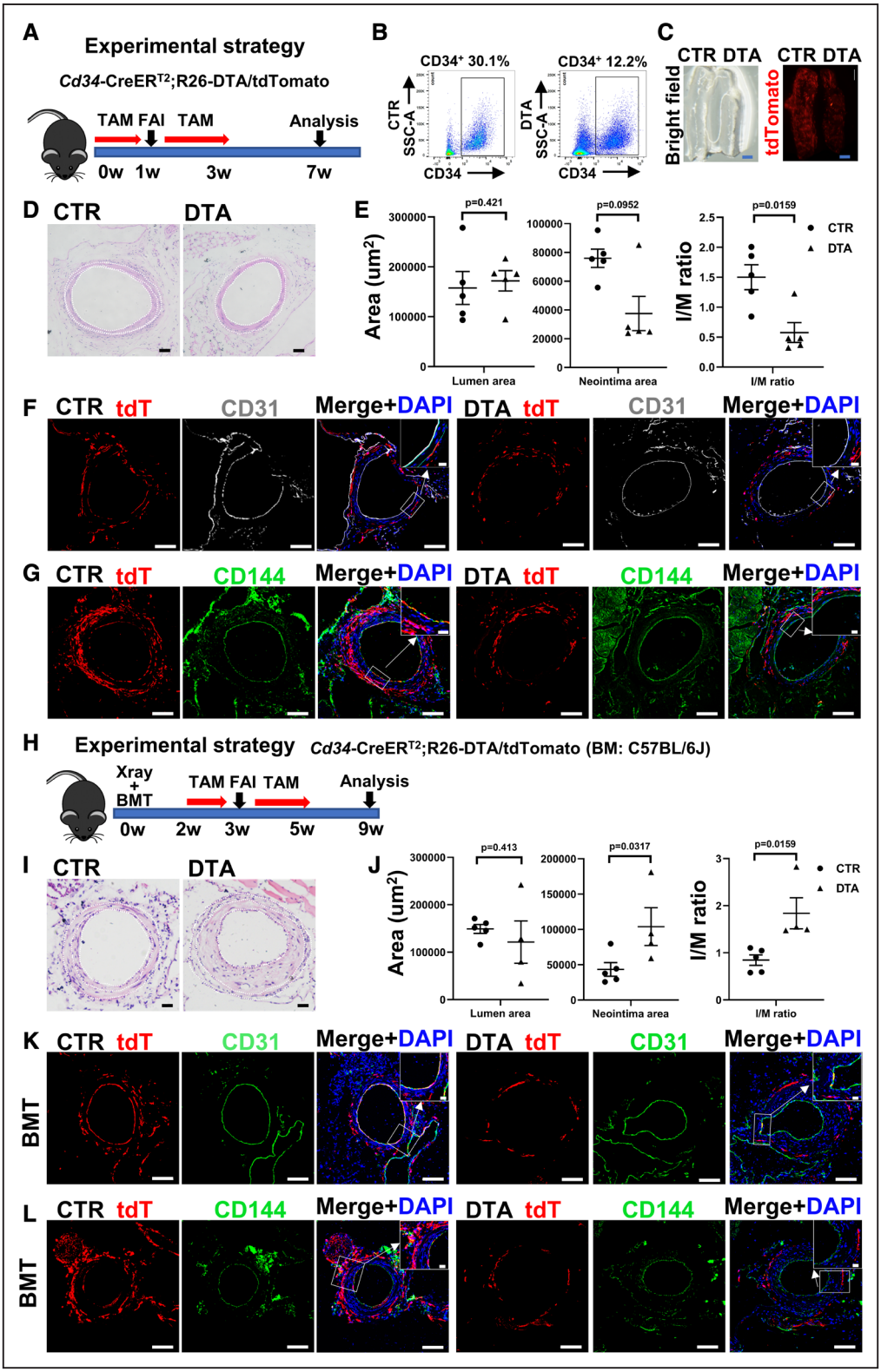

Figure 5. Depletion of CD34+ cells affects neointima formation.
A, Sketch of the experimental design for CD34+ cell depletion using *Cd34*-CreER^{T2};R26-diphtheria toxin subunit A (DTA)/tdTomato (tdT) mice. *Cd34*-CreER^{T2};R26-tdT mice were used as control mice (CTR) in following experiments. **B**, Flow cytometric analysis of CD34 expression on femoral arteries after depleting CD34+ cells. **C**, TdT fluorescence and bright-field images of femoral arteries after depleting CD34+ cells. **D**, H&E staining of femoral arteries after wire injury in CD34+ cell-ablated and CTR mice. **E**, Quantification of luminal and neointimal areas, and neointima/media (I/M) ratio after femoral artery injury (FAI) with CD34+ cell depletion. **F**, Immunostaining for tdT and CD31 on femoral artery sections from CTR mice and CD34+ cell-ablated DTA mice, with magnification of the boxed region. (*Continued*)

regulating endothelial regeneration in this vascular injury model, we further performed scRNA-seq analyses on cells from injured vessels. Femoral artery injury was performed on tamoxifen-treated *Cd34*-CreER^{T2};R26-tdTomato mice to conduct endothelial denudation. Artery samples were collected at different time points (uninjured arteries at 2 weeks after tamoxifen treatment, and 2 and 4 weeks after injury) for scRNA-seq (Figure 6A and Figure XVIIA in the Data Supplement). Femoral arteries were isolated and digested by enzymes. Single live nucleated cells were sorted out by FACS for scRNA-seq. Due to the quite small live cell number of tdTomato$^+$ cells in the samples (5.5%), we could not sort out enough tdTomato$^+$ cells for separate scRNA-seq analysis. We mixed both tdTomato$^+$ cells and tdTomato$^-$ cells to give a whole landscape of injured arteries. ScRNA-seq data from different groups were then aggregated for processing and further analyses (Figure 6B). After removing low-quality cells, a total 26 497 cells were subjected for the following analysis, including 5170 cells from uninjured wild-type C57BL/6J mouse arteries, 6704 cells from uninjured *Cd34*-CreER^{T2};R26-tdTomato mouse arteries, and 6525, as well as 8098 cells from wire-injured arteries of *Cd34*-CreER^{T2};R26-tdTomato mice at 2- and 4-week postinjury, respectively. On average, >2500 genes were detected per cell in each group (Table II in the Data Supplement).

To examine whether the *Cd34*-CreER^{T2} transgenic modification affected the gene expression of vascular cells, we first compared the cell atlas and gene expression profiles of native femoral artery cells between wild-type C57BL/6J and *Cd34*-CreER^{T2};R26-tdTomato mice. As shown in the t-distributed stochastic neighbor embedding plot, aggregated femoral artery cells comprised mesenchymal, myogenic, immune, neuronal, and ECs (Figure XVIA in the Data Supplement). Of note, the cell composition and respective percentage was similar between the 2 groups (Figure XVIB and XVIC in the Data Supplement). When examining different lineage marker genes, we observed very similar gene expression profiles between these 2 groups (Figure XVID in the Data Supplement). These data collectively suggest that cells from the genetic lineage tracing *Cd34*-CreER^{T2};R26-tdTomato mice were similar to wild-type C57BL/6J mice and could represent an exact pathophysiological process in vivo.

To depict the single-cell landscape of the vessel injury model, samples of different groups were integrated for unbiased clustering analysis. Results showed that a total of 19 cell clusters were identified (Figure 6C and Figure XVIIB and Table V in the Data Supplement), including mesenchymal cells (*Dcn*, *Pdgfra*), mural cells (*Myh11*, *Cnn1*, *Pdgfrb*), ECs (*Cdh5*, *Pecam1*), immune cells (*Ptprc*), and neurons (*Plp1*, *Sfrp5*). Among immune cell populations, we detected macrophage, monocyte/neutrophil, T cell, B cell, and dendritic cells. Samples from 4 different groups shared similar cell pattern but with different cell frequencies (Figure 6D and 6E). The percentage of SMCs and ECs decreased significantly 2 weeks postinjury to the lowest level of 10.1% and 1.0%, respectively (Figure 6E). After 4 weeks, regeneration of both cell types restored their percentage to 17.9% and 1.4%, respectively. Similar changes were also detected in mesenchymal cells (decreased to 51.8% at 2 weeks and restored to 58.5% at 4 weeks). Of note, immune cells increased substantially after wire injury and reached its peak at 2 weeks (3.0% in uninjured group, 37.0% at 2 weeks, and 22.1% at 4 weeks).

We next traced the cell fate of CD34$^+$ cells at single-cell level, by examining tdTomato$^+$ cells in our scRNA-seq data sets. Of the total 21 327 cells from *Cd34*-CreER^{T2};R26-tdTomato mice, 953 tdTomato$^+$ cells were detected and selected for further analysis (Figure XVIIC in the Data Supplement). Four different groups with 9 distinct cell clusters were identified (Figure 6F and Table VI in the Data Supplement), including immune cells (macrophages, cluster 3. T cell/dendritic cells, cluster 6. monocytes/neutrophils, cluster 9), mesenchymal cells (cluster 1, 2, 4), myogenic cells (myofibroblasts cluster 5, pericytes cluster 7) and ECs (cluster 8). They shared a similar pattern with the whole cells' data with respect to the distribution of cell components (Figure 6G and 6H and Figure XVIID in the Data Supplement). Interestingly, subgroups of mesenchymal cells were markedly changed during injury, cluster 1 dramatically increased after injury while cluster 2 and 4 significantly decreased. To verify the findings in the scRNA-seq data that CD34$^+$ cells also differentiate into myofibroblast and pericyte, which we did not examine before, we re-ran some immunostaining using the lineage tracing mice and confirmed that after vessel injury there were tdTomato$^+$ SMA$^+$

Figure 5 Continued. G, Immunostaining for tdT and CD144 on femoral artery sections from CTR mice and DTA mice, with magnification of the boxed region. **H**, Sketch of the experimental design for nonbone marrow CD34$^+$ cell depletion using chimeric DTA mice. *Cd34*-CreER^{T2};R26-DTA/tdT mice were firstly undergone wild-type (WT) bone marrow transplantation to replace their bone marrow cells by WT cells so that the bone marrow CD34$^+$ cells would not be ablated. The chimeric mice next received tamoxifen (TAM) induction to get a nonbone marrow CD34$^+$ cell depletion. *Cd34*-CreER^{T2};R26-tdT mice undergone WT bone marrow transplantation were used as CTR mice. **I**, H&E staining of femoral arteries after wire injury in nonbone marrow CD34$^+$ cell-ablated and CTR mice. **J**, Quantification of luminal and neointimal areas, and neointima/media (I/M) ratio after FAI with nonbone marrow CD34$^+$ cell depletion. **K**, Immunostaining for tdT and CD31 on femoral artery sections from CTR mice and nonbone marrow CD34$^+$ cell-ablated DTA mice, with magnification of the boxed region. **L**, Immunostaining for tdT and CD144 on femoral artery sections from CTR mice and nonbone marrow DTA mice, with magnification of the boxed region. Blue scale bars, 2 mm. Black scale bars, 50 μm. White scale bars, 100 μm and 20 μm in magnification. Data represent mean±SEM, n=5 in CTR, DTA (**E**), and CTR (**J**) groups and n=4 in the DTA (**J**) group. Data were tested by unpaired nonparametric 2-tailed Mann-Whitney *U* test. *P* values between each 2 groups were specified in the graph, $P<0.05$ was considered to be statistically significant.

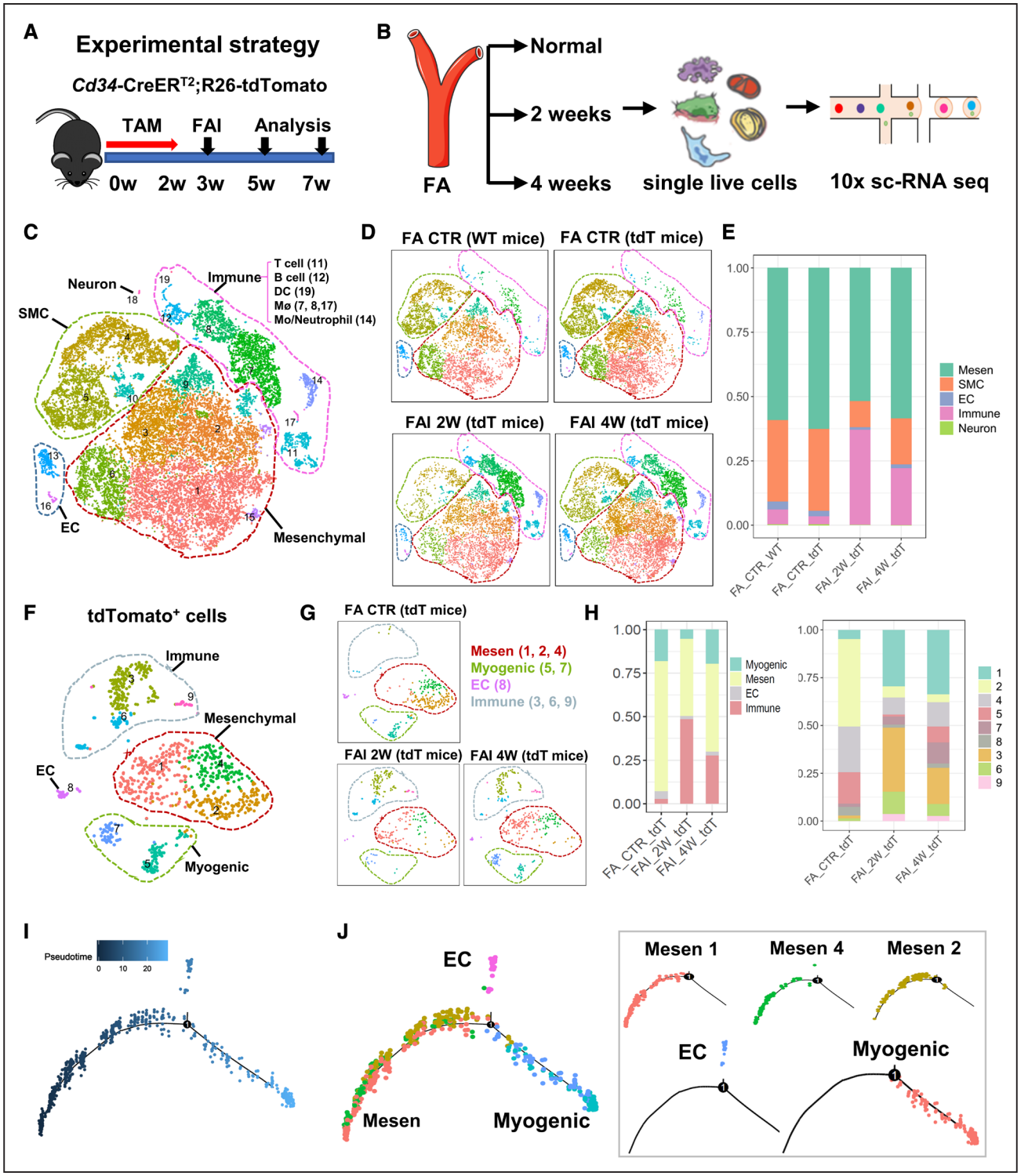

Figure 6. Single-cell RNA sequencing (scRNA-seq) analyses of cellular compositions in injured femoral arteries.
A, Sketch of the experimental design for femoral artery injury (FAI). **B**, Schematic showing scRNA-seq strategy for FAI samples. **C**, T-SNE (t-distributed stochastic neighbor embedding) plot showing the unsupervised clustering of 26 497 cells isolated from femoral arteries of all time points. **D**, Split view of 4 different groups of samples. CTR indicates uninjured artery, tdT indicates *Cd34*-CreER^{T2};R26-tdTomato mice. **E**, Bar chart showing the proportion of major cell types across samples. **F**, T-SNE plot showing the clustering of 953 tdT$^+$ cells from CD34 lineage. **G**, Split view of 3 different groups of samples. **H**, Bar charts showing the proportion of major cell types and each cell clusters across tdT$^+$ cells. **I**, Pseudotime trajectory analysis of mesenchymal cells, mural cells, and endothelial cells (ECs), color by pseudotime. **J**, Trajectory analysis of mesenchymal cells, mural cells, and ECs, color by cell clusters. Split view of trajectory analysis of each cluster was shown on the **right**.

PDGFRa+ myofibroblasts and tdTomato+ NG2+ PDGFRb+ pericytes in the adventitia (Figure XVIIE and XVIIF in the Data Supplement).

We also investigated the chemokine expression patterns and explored possible intercellular communications inside the tdTomato+ cell population. The immune cell clusters exhibited most active chemokine interaction, and the mesenchymal population was the second active cell type. Based on the expression pattern, we analyzed the top signature ligand-receptor pairs and revealed the CXCL12-ITGB1 interaction was the major pattern in the crosstalk between CD34-derived mesenchymal and EC populations (Figures XVIII and XIXA in the Data Supplement), especially after vascular injury (Figure XIXB in the Data Supplement).

Our data above had revealed that immune cells were generated from BM source of CD34+ cells, the relationship among mesenchymal cells, ECs, and myogenic cells, which were the non-BM source, were still unclear. Gene marker of EC (*Pecam1*/CD31) was restricted in the EC population in both the whole cell and the tdTomato+ cell data sets (Figure XXA and XXB in the Data Supplement). To test a possibility of mesenchymal cells differentiation into ECs or myogenic cells, we performed pseudotime analysis using the Monocle R package,[30–32] and ordered mesenchymal cells, myogenic cells, and ECs along a trajectory (Figure 6I). Two groups of mesenchymal cells abundant in the normal femoral artery were found at the left half of a trajectory, while ECs and myogenic cells were located at 2 distinct ends of the trajectory. Interestingly, subgroups of mesenchymal cells enriched in injured vessels were found in different time periods, cluster 1 and 4 mainly appeared in the initial phase while cluster 2 mainly in the middle period closer to the branch point, suggesting a transitional state of these cells and a possible differentiation from CD34+ mesenchymal cells to ECs or myogenic cells. Analysis of the branch point uncovered upregulated gene blocks (gene module 1) toward EC, with EC marker genes *Cdh5* and *Vwf*. Myogenic marker genes *Acta2* and *Rgs5* were shown upregulated in gene module 2, with the cell trajectory toward myogenic cells (Figure XXC in the Data Supplement). Of note, progenitor makers *Ly6a* and *Cd34* were detected in gene module 3 in the prebranch part, indicating an immature state and a tendency of differentiation. Gene enrichment analysis for genes in module 3 revealed enriched expression for vasculature development (Figure XXD in the Data Supplement).

Vascular Adventitial CD34+ Cells Display Endothelial Differentiation Potential In Vitro

Our scRNA-seq data suggested a possible role of vascular resident adventitial CD34+ mesenchymal cells in endothelial regeneration. Despite the cellular heterogeneity of CD34+ cells as described above, we supposed that vascular CD34+ cells may possess a higher potential to differentiate into ECs. To test this hypothesis, we isolated vascular adventitial CD34+ cells from mouse aorta using a magnetic-activated cell sorting protocol (Figure XXIA in the Data Supplement) as previously described.[17,27] Phenotypic analysis by flow cytometry confirmed that most isolated cells were CD34+ (Figure XXIB in the Data Supplement). CD34+ cells were then cultured in EGM-2 (endothelial cell growth medium-2) to test differentiation potential. After 3 to 7 days of culture, endothelial-specific genes (*Cdh5* encoding protein CD144, *Pecam1* encoding protein CD31, *Kdr* encoding protein VEGFR2, and *Nos3* encoding protein eNOS) were significantly increased over time (Figure XXIC in the Data Supplement). Immunofluorescence also displayed the typical cobblestone morphology of ECs and the increase of endothelial markers CD144 and eNOS (Figure XXID in the Data Supplement), while expression of *Cd34* was significantly decreased (Figure XXIE in the Data Supplement). Collectively, these data demonstrate the differentiation potential of vascular adventitial CD34+ cells into ECs in vitro.

MiR-21-Smad7-pSmad2/3 Pathway Regulates Endothelial Differentiation

We next sought to reveal the underlying mechanism of CD34+ cell differentiating into ECs. By evaluating several key miR, we found that miR-21 was increased significantly during endothelial differentiation from adventitial CD34+ cells (Figure XXIF in the Data Supplement). We next used mimics or inhibitor to overexpress or knockdown miR-21. Our results showed that overexpression of miR-21 strongly upregulated the expression of canonical endothelial markers *Cdh5* and *Pecam1*, while knockdown of miR-21 significantly decreased them (Figure 7A). Functionally, overexpression of miR-21 promoted tube formation of the CD34+ cells-derived ECs (Figure XXIG in the Data Supplement).

To reveal the miR-21 related molecular mechanism in adventitia CD34+ cell differentiation, we used R package SCENIC[33] to evaluate the regulatory network in tdTomato+ cell population. Several key transcriptional factors were identified and TGF (transforming growth factor)-β pathway relevant *Foxp2* was characterized in mesenchymal populations (Figure XXIIA in the Data Supplement). To validate if TGF-β pathway was actually related to the differentiation process, we re-ran the trajectory analyses in our tdTomato+ cell data set. Using the TRRUST database[34] to predict the transcriptional regulatory network we found several key transcriptional modulators including *Sp1* and *Smad3* (Figure XXIIB in the Data Supplement), which indicated that the TGF-β signaling pathway was involved in the differentiating process. In the TGF-β signaling pathway, several factors were involved in EC differentiation including *Tgfb1*, *Smad1*, *Smad6*, *Smad7*,

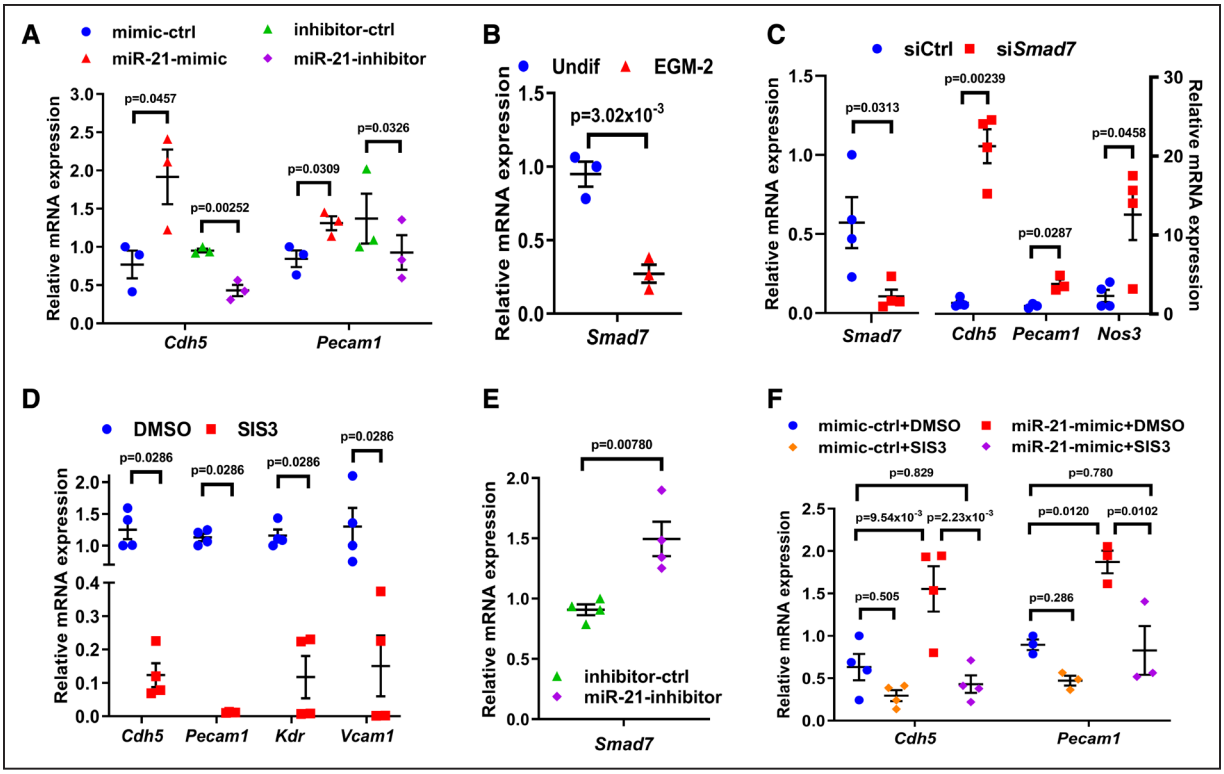

Figure 7. Smad7-pSmad2/3 pathway, negatively regulated by microRNA-21 (miR-21), regulates endothelial gene expression and function during CD34+ cells differentiating into endothelial cells (ECs).

A, Quantitative polymerase chain reaction (PCR) analyses of EC genes *Cdh5* and *Pecam1* using miR-21 mimic or inhibitor, n=3 per group. **B**, Quantitative PCR analyses of *Smad7* expression in adventitia CD34+ cell differentiating into ECs, n=3 in each group. **C**, Quantitative PCR analyses of EC genes expression after knocking down *Smad7* with siRNA, n=4 or 3 (*Pecam1*) per group. **D**, Quantitative PCR analyses of EC markers expression in adventitia CD34+ cells with pSmad2/3 inhibition, n=4 per group. **E**, Quantitative PCR analyses of *Smad7* expression with miR-21 inhibitor, n=4 in each group. **F**, Quantitative PCR analyses of EC genes with miR-21 mimic and pSmad2/3 inhibitor (SIS3), n=4 (*Cdh5*) or 3 (*Pecam1*). Data represent mean±SEM. Data were first tested by Shapiro-Wilk test for normality. Normally distributed data were then tested by unpaired 2-tailed *t* test between groups without or with Welch correction if uneven variances existed (**A**–**C**, **E**), or by 1-way ANOVA with Tukey test (**F**). Non-normally distributed data were examined by unpaired Mann-Whitney *U* test (**D**). *P* values between each 2 groups were specified in the graph, $P<0.05$ was considered to be statistically significant. Ctrl indicates control; and Undif, undifferentiated medium.

and *Mapk3*. *Mapk1*, *Tgfb2*, and *Mtor* were involved in myogenic differentiation while some unchanged factors were also detected in the last gene module (Figure XXIIC in the Data Supplement).

As a direct gene target of miR-21 and a key modulator in the TGF-β pathway, *Smad7* was characterized in the trajectory and had been reported to suppresses EC differentiation and angiogenesis via inhibiting Smad2/3 phosphorylation.[35] We, therefore, focused on Smad7 and tested its potential role in our in vitro experiments. *Smad7* was downregulated during adventitial CD34+ cell differentiation (Figure 7B). Knockdown of *Smad7* with siRNA promoted adventitial CD34+ cells differentiating into ECs, with notably increased expression of endothelial markers (Figure 7C). The silencing of *Smad7* also enhanced the capacity of tube formation of adventitial CD34+ cells (Figure XXIID in the Data Supplement). Since intracellular transduction of TGF-β depends on Smad2/3 phosphorylation, we further used SIS3, an inhibitor that suppresses the phosphorylation of Smad2/3, to examine their impact on endothelial differentiation. As expected, suppression of Smad2/3 phosphorylation in adventitial CD34+ cells significantly decreased expression of endothelial markers (Figure 7D), as well as decreased tube formation and LDL (low-density lipoprotein) uptake capacities (Figure XXIIE in the Data Supplement), suggesting an essential role of the Smad7-pSmad2/3 axis in endothelial differentiation from adventitial CD34+ cells.

We then examined whether miR-21 promotes endothelial differentiation by modulating Smad7-pSmad2/3 pathway. By using miR-21 inhibitors, we found that miR-21 indeed negatively regulated Smad7 expression (Figure 7E). Since the Smad7-pSmad2/3 pathway was established, we next examined whether miR-21 affects endothelial differentiation of by targeting Smad2/3. Inhibiting Smad2/3 phosphorylation with SIS3 abolished the prodifferentiation effect of miR-21, as evidenced by decreased expression of endothelial markers *Cdh5* and *Pecam1* (Figure 7F). Thus, our data established that miR-21 is involved in regulating the differentiation of adventitial CD34+ cells into the ECs

via negatively modulating Smad7-pSmad2/3 pathway (Figure XXIIF in the Data Supplement).

DISCUSSION

Since the isolation of CD34+ putative EPCs from peripheral blood mononuclear cells,[36] CD34+ cell therapy has been tested in lots of clinical studies to treat cardiovascular diseases.[37,38] However, outcomes of these clinic trials varied tremendously,[39,40] and soon hindered the translation of such therapy into clinical practice. Several recent studies have indicated the presence of tissue-resident CD34+ cells, especially in the vessel wall,[17–19] but their precise origin and role in endothelial regeneration remains unclear. Our study of human healthy and diseased arteries showed increased CD34-expressing cells in pathological conditions, revealing a potential impact of CD34+ cells on vessel diseases. We next combined the use of scRNA-seq and genetic lineage tracing technology and uncovered vascular CD34+ cells as a heterogeneous population that contributes to endothelial repair after vascular injury. First, we depicted a single-cell transcriptomic landscape of normal and injured femoral arteries, in which distinct and heterogeneous populations of CD34+ cells were found. Second, by tracing *Cdh5*+ ECs and *Cd34*+ cells we revealed that at the centric region of injured area the Cd34+ mesenchymal cells were responsible for endothelial regeneration rather than preexiting ECs. Third, we provided solid evidence that BM CD34+ cells primarily contributed to inflammatory response, resembling the function of BM c-Kit+ cells as previously reported,[26,27] while non-BM CD34+ cells were responsible for endothelial regeneration after vessel injury. Fourth, different origins of CD34+ cells exhibited distinct pathological responses that partially ablating non-BM CD34+ cells aggravated neointimal lesions. Finally, we elucidated a possible mechanism of vascular adventitial CD34+ cell differentiation into the endothelial lineage. Taken together, our findings provide the fundamental information for the heterogeneity of CD34+ cells and establish their pathological significance in endothelial regeneration, offering a potential therapeutic target for treating vascular diseases.

Recently, a number of scRNA-seq studies have been published and featured cellular diversity in the vessel wall.[41–44] While most of these studies have focused on the aorta, our scRNA-seq data were specially designed to explore the cell atlas of the mouse femoral artery under both physiological and pathological conditions and provide additional transcriptomic information of different types of arteries. Interestingly, our scRNA-seq analyses have revealed distinct cell clusters in the femoral artery when compared with previous scRNA-seq studies of the aorta. By further using scRNA-seq and genetic lineage tracing model, we demonstrated the expression of CD34 in a heterogeneous population in the mouse femoral artery, including a large population of adventitial mesenchymal cells, a small group of ECs and immune cells. Although in scRNA-seq data we identified myogenic cells, we did not observe them in FACS sorted protein CD34+ scRNA-seq data or any tdTomato+ SMCs in immunostaining, which may due to low expression level of mRNAs and lack of protein translation.

In the mouse endothelial denudation injury model, a large number of CD34-derived ECs were identified in the inner layer of lumen and in the adventitia, supporting that CD34+ cells give rise to both artery and microvessel ECs. By comparing to the results acquired from the *Cdh5*-lineage tracing mice, these CD34+ cells, mostly responsible for the centric region regeneration and adventitia microvessel expansion in the injured artery, were from a nonmature EC source. Besides, our scRNA-seq data from the CD34 lineage traced mice also identified ECs in tdTomato-expressing cells. Recent studies have revealed a mesenchymal-to-endothelial transition in peripheral ischemia, cardiac diseases, and tumor growth,[45–48] our study provides a novel insight that this transition may also take place in vascular diseases and raise a new source for endothelial regeneration. Besides, as previous studies have indicated, adventitial Sca-1+/c-Kit+ cells are shown to differentiate into SMCs but not CD34+ cells.[49,50] In our model, CD34+ cells still do not regenerate neointimal SMCs but contributed to adventitia myofibroblasts and pericytes.

By examining the role of CD34+ cells in the femoral artery under both normal and diseased condition, we elucidated the exact biological identity and the heterogeneity of CD34+ cell population, which may largely explain why CD34+ cell-based clinical therapies produced different outcomes. According to the results of randomized trials using Combo stents (combine CD34 antibody and conventional anti-proliferative drugs), many of trials failed to achieve superior outcomes from this stent, to both the second (REMEDEE [randomized study to evaluate the safety and effectiveness of an abluMinal sirolimus coatED bio-Engineered StEnt] and HARMONEE [harmonized assessment by randomized multicentre study of orbusNEich's combo StEnt] studies[51–53]) and third (SORT OUT X trial [Scandinavian Organization for Randomized Trials with Clinical Outcome X- Combo Stent Versus Orsiro Stent][14]) generations of stents but rather led to an even higher frequency of uncovered stent struts than conventional stents.[54] This could be explained by the heterogeneity of CD34+ cells, as BM derived CD34+ cells exaggerate inflammatory response in injured vessels and enhance lesion formation. According to our results using 2 kinds of diphtheria toxin-induced cell ablating systems, depleting all CD34+ cells resulted in a decrease of neointima formation while ablating non-BM source of CD34+ cells exacerbated it, indicating a proatherosclerotic role of BM-originated CD34+ cell-mediated inflammation. Therefore, CD34 antibody may capture a mixed cell population in these stents, in which the majority may be BM CD34+ cells that would eventually convert to immune cells.[12,13] To improve the clinical efficacy of combo stents, a novel method to specifically recruit or capture non-BM CD34+ cells may be developed and to combine with certain drugs to induce their differentiation into ECs.

While our study demonstrated that non-BM CD34+ cells regenerate ECs in vivo, we also noticed that CD34+ cells give rise to both luminal ECs in the neointima and microvessel ECs in adventitia after femoral artery injury. Luminal ECs maintain vessel integrity and protect against neointima formation,[55] while under diseased conditions, the expansion of microvessels in both the neointima and adventitia is associated with atherosclerotic plaque growth and progression.[56] Thus, it would also be interesting to distinguish and characterize the luminal and microvessel CD34-derived ECs. This information may help to develop the therapeutic approach aimed at the regression of the microvessels and restoration to the normal architecture of blood vessel.

Despite clear evidence for the non-BM origin of CD34-derived ECs, the exact origin of these cells remains unknown. We proposed that CD34+ cells from the adventitia may be possible sources, as evidenced by our *en-face* staining and in vitro data that adventitial CD34+ mesenchymal cells displayed endothelial differentiation potential. Other tissues have been reported to harbor resident progenitor cells, including perivascular tissue, adipose tissue, spleen, and liver, can also be a possible source of these CD34-derived ECs. Besides, a small number of ECs may also reenter cell cycle, re-gain CD34 expression, and contribute to endothelial regeneration. Consistent with previous findings that ECs are a heterogeneous population and harbor a stem/progenitor population, lineage tracing studies have also identified possible vascular EPCs such as CD31^{hi}Emcn^{hi} cell,[57] and CD34+CD31^{lo}VEGFR2^{-} endovascular progenitor.[58] Recent scRNA-seq studies of the aorta have also confirmed the heterogeneity of ECs.[42,59,60] By using spatial transcriptomics, which enables the direct observation of intimal and adventitial cells, and dual recombinase system, we may be more specific in labeling and tracing the fate of distinct subpopulations of CD34+ cells, including luminal, microvessel, and nonendothelial CD34+ cells. Moreover, although our results indicated a role of CD34+ cells in artery endothelial regeneration, it should be noted that CD34+ cells generated only half of the de novo ECs. Identification and characterization of alternative sources of ECs warrant further study.

Although early works showed that vascular adventitial CD34+ cells can differentiate into ECs, the underlying mechanisms remain unclear. We detected a significant increase of miR-21 in the differentiation of CD34+ cells to ECs, which has been recently found to impact cardiovascular pathology and could stimulate endothelial proliferation, but their target genes were not clear.[61] By regulatory network analyses, we showed that the TGF-β pathway was involved in EC pathophysiology after vessel injury. Smad7-pSmad2/3 is a known modulator in the TGF-β pathway and a miR-21 target and plays a role in angiogenesis.[62] However, previous studies on these molecules usually investigated them on SMC and ECs,[63] seldom studies investigated them on iPSCs (induced pluripotent stem cells).[61] Here, we proposed a possible mechanism, in which a miR-21-Smad7-pSmad2/3 pathway regulates the differentiation of adventitia CD34+ cells into ECs and vascular angiogenesis. Therefore, we provide direct evidence on the pathways leading to vascular adventitial CD34+ cell differentiating into EC in vitro. The adventitial CD34+ cells isolated in our study is still a heterogenous population, future work using multiple modern methods including scRNA-seq to find more precise markers and characterize the true progenitor population is needed for a more efficient in vitro/in vivo transdifferentiation of CD34+ cells.

Although our in vitro study suggests a possible role of vascular adventitial CD34+ cell differentiating into ECs, our scRNA-seq data also showed a small group of CD34+ ECs in the femoral artery. This observation was consistent with our findings in the femoral artery staining that CD34-high-expressing cells consisted a quite small population in the intimal layer. Atherosclerotic lesions in humans are abundant for CD34+ ECs, indicating that some findings from mouse models could be validated in humans. By comparing the FACS sorted CD34+ ECs and gene *Cd34*$^{-}$ ECs, it revealed that CD34+ ECs are a much more active component in the endothelium.

In summary, our findings demonstrate diverse roles of CD34+ cells after wire-induced endothelial denudation, in which CD34+ cell-conducted endothelial regeneration was involved. Rapid luminal endothelial regeneration promoted wound healing, while inflammatory cells contribute to the progression of neointimal hyperplasia. It should be noted that in our present data, we selectively deplete CD34+ cells from BM or non-BM sources, but the contribution of each CD34+ subpopulation remains unclear. To explore their respective roles in this diseased vessel, we may further combine dual recombinase system and cell ablating models. The combined genetic and bioinformatic evidence of vascular CD34+ cells might provide insight into endothelial progenitors and contribute to a promising therapeutic approach for vascular diseases.

ARTICLE INFORMATION

Received May 7, 2021; revision received August 22, 2021; accepted September 1, 2021.

Affiliations

Department of Cardiology, the First Affiliated Hospital, Zhejiang University School of Medicine, Hangzhou, Zhejiang Province, China (L. Jiang, T. Chen, S. Sun, R. Wang, J. Deng, L. Lyu, H. Wu, X. Pu, L. Du, Y. Hu, X. Hu, Y. Zhou, Q. Xu). Department of Cardiology and Institute for Developmental and Regenerative Cardiovascular Medicine, Xinhua Hospital Affiliated to Shanghai Jiaotong University School of Medicine, Shanghai, China. (S. Sun, M. Yang, Q. Chen, L. Zhang) . Alibaba-Zhejiang University Joint Research Center of Future Digital Healthcare, Hangzhou, Zhejiang Province, China (T. Chen). Centre for Clinical Pharmacology, William Harvey Research Institute, Queen Mary University of London, London, United Kingdom (Q. Xu).

Acknowledgments

This work was supported by Alibaba-Zhejiang University Joint Research Center of Future Digital Healthcare and Alibaba Cloud. We are also grateful to the Core Facility Platform of Zhejiang University School of Medicine for technical assistance. Q. Xu and L. Zhang conceived ideas and designed the research. L. Jiang, T. Chen, S. Sun, R. Wang, J. Deng, Y. Zhou, and L. Lyu performed single-cell RNA sequencing (scRNA-seq), L. Jiang, J. Deng, and Q. Chen analyzed scRNA-seq data. L. Jiang, S. Sun, R. Wang, Y. Hu, X. Hu, H. Wu, M. Yang, X. Pu, and L. Du performed animal experiments, flow cytometric experiments, and immunostaining.

T. Chen performed in vitro work. L. Jiang, T. Chen, S. Sun, and Q. Xu created the figures and wrote the article. T. Chen, Q. Xu and L. Zhang acquired funding. All authors contributed to the article.

Sources of Funding

This work was supported by a grant from the National Key R&D Program of China (2018YFE0200503), grants from the National Natural Science Foundation of China (31830039, 81770435, 81930010, 82030008, 81800364 and 81870206), a grant from the Natural Science Foundation of Zhejiang Province (LD18H020001) and a grant from the Shanghai "Rising Stars of Medical Talent" Youth Development Program "Outstanding Youth Medical Talents" (SHWSRS(2021)_099).

Disclosures

None.

Supplemental Materials

Expanded Materials & Methods
Data Supplement Figures I–XXII
Data Supplement Tables I–IX
Major Resources Table
Graphic abstract
References[25–27,30–34,61,64–72]

REFERENCES

1. Ross R. The pathogenesis of atherosclerosis — an update. *N Engl J Med*. 1986;314:488-500. doi: 10.1056/NEJM198602203140806
2. Krause DS, Fackler MJ, Civin CI, May WS. CD34: structure, biology, and clinical utility. *Blood*. 1996;87:1–13. doi: 10.1182/blood.V87.1.1.1
3. Zhang L, Issa Bhaloo S, Chen T, Zhou B, Xu Q. Role of resident stem cells in vessel formation and arteriosclerosis. *Circ Res*. 2018;122:1608–1624. doi: 10.1161/CIRCRESAHA.118.313058
4. Asahara T, Murohara T, Sullivan A, Silver M, van der Zee R, Li T, Witzenbichler B, Schatteman G, Isner JM. Isolation of putative progenitor endothelial cells for angiogenesis. *Science*. 1997;275:964–967. doi: 10.1126/science.275.5302.964
5. Zhu JH, Wang XX, Zhang FR, Shang YP, Tao QM, Zhu JH, Chen JZ. Safety and efficacy of autologous endothelial progenitor cells transplantation in children with idiopathic pulmonary arterial hypertension: open-label pilot study. *Pediatr Transplant*. 2008;12:650–655. doi: 10.1111/j.1399-3046.2007.00863.x
6. Lara-Hernandez R, Lozano-Vilardell P, Blanes P, Torreguitart-Mirada N, Galmés A, Besalduch J. Safety and efficacy of therapeutic angiogenesis as a novel treatment in patients with critical limb ischemia. *Ann Vasc Surg*. 2010;24:287–294. doi: 10.1016/j.avsg.2009.10.012
7. Jimenez-Quevedo P, Gonzalez-Ferrer JJ, Sabate M, Garcia-Moll X, Delgado-Bolton R, Llorente L, Bernardo E, Ortega-Pozzi A, Hernandez-Antolin R, Alfonso F, et al. Selected CD133⁺ progenitor cells to promote angiogenesis in patients with refractory angina: final results of the PROGENITOR randomized trial. *Circ Res*. 2014;115:950–960. doi: 10.1161/CIRCRESAHA.115.303463
8. Tanaka R, Masuda H, Kato S, Imagawa K, Kanabuchi K, Nakashioya C, Yoshiba F, Fukui T, Ito R, Kobori M, et al. Autologous G-CSF-mobilized peripheral blood CD34+ cell therapy for diabetic patients with chronic nonhealing ulcer. *Cell Transplant*. 2014;23:167–179. doi: 10.3727/096368912X658007
9. Zhu J, Song J, Yu L, Zheng H, Zhou B, Weng S, Fu G. Safety and efficacy of autologous thymosin β4 pre-treated endothelial progenitor cell transplantation in patients with acute ST segment elevation myocardial infarction: a pilot study. *Cytotherapy*. 2016;18:1037–1042. doi: 10.1016/j.jcyt.2016.05.006
10. D'Avola D, Fernández-Ruiz V, Carmona-Torre F, Méndez M, Pérez-Calvo J, Prósper F, Andreu E, Herrero JI, Iñarrairaegui M, Fuertes C, et al. Phase 1-2 pilot clinical trial in patients with decompensated liver cirrhosis treated with bone marrow-derived endothelial progenitor cells. *Transl Res*. 2017;188:80–91.e2. doi: 10.1016/j.trsl.2016.02.009
11. Vasyliev RG, Oksymets VM, Rodnichenko AE, Zlatska AV, Gubar OS, Gordiienko IM, Zubov DO. Tissue-engineered bone for treatment of combat related limb injuries. *Exp Oncol*. 2017;39:191–196. doi: 10.31768/2312-8852.2017.39(3):191.196
12. Aoki J, Serruys PW, van Beusekom H, Ong AT, McFadden EP, Sianos G, van der Giessen WJ, Regar E, de Feyter PJ, Davis HR, et al. Endothelial progenitor cell capture by stents coated with antibody against CD34: the HEALING-FIM (Healthy Endothelial Accelerated Lining Inhibits Neointimal Growth-First In Man) Registry. *J Am Coll Cardiol*. 2005;45:1574–1579. doi: 10.1016/j.jacc.2005.01.048
13. Rotmans JI, Heyligers JM, Verhagen HJ, Velema E, Nagtegaal MM, de Kleijn DP, de Groot FG, Stroes ES, Pasterkamp G. In vivo cell seeding with anti-CD34 antibodies successfully accelerates endothelialization but stimulates intimal hyperplasia in porcine arteriovenous expanded polytetrafluoroethylene grafts. *Circulation*. 2005;112:12–18. doi: 10.1161/CIRCULATIONAHA.104.504407
14. Jakobsen L, Christiansen EH, Freeman P, Kahlert J, Veien K, Maeng M, Raungaard B, Ellert J, Villadsen AB, Kristensen SD, et al. Randomized clinical comparison of the dual-therapy CD34 antibody-covered sirolimus-eluting combo stent with the sirolimus-eluting orsiro stent in patients treated with percutaneous coronary intervention: The SORT OUT X Trial. *Circulation*. 2021;143:2155–2165. doi: 10.1161/CIRCULATIONAHA.120.052766
15. Prokopi M, Pula G, Mayr U, Devue C, Gallagher J, Xiao Q, Boulanger CM, Westwood N, Urbich C, Willeit J, et al. Proteomic analysis reveals presence of platelet microparticles in endothelial progenitor cell cultures. *Blood*. 2009;114:723–732. doi: 10.1182/blood-2009-02-205930
16. Yoder MC. Is endothelium the origin of endothelial progenitor cells? *Arterioscler Thromb Vasc Biol*. 2010;30:1094–1103. doi: 10.1161/ATVBAHA.109.191635
17. Hu Y, Zhang Z, Torsney E, Afzal AR, Davison F, Metzler B, Xu Q. Abundant progenitor cells in the adventitia contribute to atherosclerosis of vein grafts in ApoE-deficient mice. *J Clin Invest*. 2004;113:1258–1265. doi: 10.1172/JCI19628
18. Ingram DA, Mead LE, Moore DB, Woodard W, Fenoglio A, Yoder MC. Vessel wall-derived endothelial cells rapidly proliferate because they contain a complete hierarchy of endothelial progenitor cells. *Blood*. 2005;105:2783–2786. doi: 10.1182/blood-2004-08-3057
19. Zengin E, Chalajour F, Gehling UM, Ito WD, Treede H, Lauke H, Weil J, Reichenspurner H, Kilic N, Ergün S. Vascular wall resident progenitor cells: a source for postnatal vasculogenesis. *Development*. 2006;133:1543–1551. doi: 10.1242/dev.02315
20. Bearzi C, Leri A, Lo Monaco F, Rota M, Gonzalez A, Hosoda T, Pepe M, Qanud K, Ojaimi C, Bardelli S, et al. Identification of a coronary vascular progenitor cell in the human heart. *Proc Natl Acad Sci USA*. 2009;106:15885–15890. doi: 10.1073/pnas.0907622106
21. Fang S, Wei J, Pentinmikko N, Leinonen H, Salven P. Generation of functional blood vessels from a single c-kit+ adult vascular endothelial stem cell. *PLoS Biol*. 2012;10:e1001407. doi: 10.1371/journal.pbio.1001407
22. Naito H, Kidoya H, Sakimoto S, Wakabayashi T, Takakura N. Identification and characterization of a resident vascular stem/progenitor cell population in preexisting blood vessels. *EMBO J*. 2012;31:842–855. doi: 10.1038/emboj.2011.465
23. Majka SM, Jackson KA, Kienstra KA, Majesky MW, Goodell MA, Hirschi KK. Distinct progenitor populations in skeletal muscle are bone marrow derived and exhibit different cell fates during vascular regeneration. *J Clin Invest*. 2003;111:71–79. doi: 10.1172/JCI16157
24. Tintut Y, Alfonso Z, Saini T, Radcliff K, Watson K, Boström K, Demer LL. Multilineage potential of cells from the artery wall. *Circulation*. 2003;108:2505–2510. doi: 10.1161/01.CIR.0000096485.64373.C5
25. Stuart T, Butler A, Hoffman P, Hafemeister C, Papalexi E, Mauck WM 3rd, Hao Y, Stoeckius M, Smibert P, Satija R. Comprehensive integration of single-cell data. *Cell*. 2019;177:1888–1902.e21. doi: 10.1016/j.cell.2019.05.031
26. Chen Q, Yang M, Wu H, Zhou J, Wang W, Zhang H, Zhao L, Zhu J, Zhou B, Xu Q, et al. Genetic lineage tracing analysis of c-kit+ stem/progenitor cells revealed a contribution to vascular injury-induced neointimal lesions. *J Mol Cell Cardiol*. 2018;121:277–286. doi: 10.1016/j.yjmcc.2018.07.252
27. Ni Z, Deng J, Potter CMF, Nowak WN, Gu W, Zhang Z, Chen T, Chen Q, Hu Y, Zhou B, et al. Recipient c-Kit lineage cells repopulate smooth muscle cells of transplant arteriosclerosis in mouse models. *Circ Res*. 2019;125:223–241. doi: 10.1161/CIRCRESAHA.119.314855
28. Wang H, Zhao H, Zhu H, Li Y, Tang J, Li Y, Zhou B. Sca1+ cells minimally contribute to smooth muscle cells in atherosclerosis. *Circ Res*. 2021;128:133–135. doi: 10.1161/CIRCRESAHA.120.317972
29. Ivanova A, Signore M, Caro N, Greene ND, Copp AJ, Martinez-Barbera JP. In vivo genetic ablation by cre-mediated expression of diphtheria toxin fragment A. *Genesis*. 2005;43:129–135. doi: 10.1002/gene.20162
30. Trapnell C, Cacchiarelli D, Grimsby J, Pokharel P, Li S, Morse M, Lennon NJ, Livak KJ, Mikkelsen TS, Rinn JL. The dynamics and regulators of cell fate decisions are revealed by pseudotemporal ordering of single cells. *Nat Biotechnol*. 2014;32:381–386. doi: 10.1038/nbt.2859

31. Qiu X, Hill A, Packer J, Lin D, Ma YA, Trapnell C. Single-cell mRNA quantification and differential analysis with census. *Nat Methods*. 2017;14:309–315. doi: 10.1038/nmeth.4150
32. Qiu X, Mao Q, Tang Y, Wang L, Chawla R, Pliner HA, Trapnell C. Reversed graph embedding resolves complex single-cell trajectories. *Nat Methods*. 2017;14:979–982. doi: 10.1038/nmeth.4402
33. Aibar S, González-Blas CB, Moerman T, Huynh-Thu VA, Imrichova H, Hulselmans G, Rambow F, Marine JC, Geurts P, Aerts J, et al. SCENIC: single-cell regulatory network inference and clustering. *Nat Methods*. 2017;14:1083–1086. doi: 10.1038/nmeth.4463
34. Han H, Cho JW, Lee S, Yun A, Kim H, Bae D, Yang S, Kim CY, Lee M, Kim E, et al. TRRUST v2: an expanded reference database of human and mouse transcriptional regulatory interactions. *Nucleic Acids Res*. 2018;46:D380–D386. doi: 10.1093/nar/gkx1013
35. Li X, Sun X, Carmeliet P. Hallmarks of endothelial cell metabolism in health and disease. *Cell Metab*. 2019;30:414–433. doi: 10.1016/j.cmet.2019.08.011
36. Asahara T, Masuda H, Takahashi T, Kalka C, Pastore C, Silver M, Kearne M, Magner M, Isner JM. Bone marrow origin of endothelial progenitor cells responsible for postnatal vasculogenesis in physiological and pathological neovascularization. *Circ Res*. 1999;85:221–228. doi: 10.1161/01.res.85.3.221
37. Marvasti TB, Alibhai FJ, Weisel RD, Li RK. CD34+ stem cells: promising roles in cardiac repair and regeneration. *Can J Cardiol*. 2019;35:1311–1321. doi: 10.1016/j.cjca.2019.05.037
38. Prasad M, Corban MT, Henry TD, Dietz AB, Lerman LO, Lerman A. Promise of autologous CD34+ stem/progenitor cell therapy for treatment of cardiovascular disease. *Cardiovasc Res*. 2020;116:1424–1433. doi: 10.1093/cvr/cvaa027
39. Schächinger V, Erbs S, Elsässer A, Haberbosch W, Hambrecht R, Hölschermann H, Yu J, Corti R, Mathey DG, Hamm CW, et al; REPAIR-AMI Investigators. Improved clinical outcome after intracoronary administration of bone-marrow-derived progenitor cells in acute myocardial infarction: final 1-year results of the REPAIR-AMI trial. *Eur Heart J*. 2006;27:2775–2783. doi: 10.1093/eurheartj/ehl388
40. Sürder D, Manka R, Moccetti T, Lo Cicero V, Emmert MY, Klersy C, Soncin S, Turchetto L, Radrizzani M, Zuber M, et al. Effect of bone marrow-derived mononuclear cell treatment, early or late after acute myocardial infarction: twelve months CMR and long-term clinical results. *Circ Res*. 2016;119:481–490. doi: 10.1161/CIRCRESAHA.116.308639
41. Gu W, Ni Z, Tan YQ, Deng J, Zhang SJ, Lv ZC, Wang XJ, Chen T, Zhang Z, Hu Y, et al. Adventitial cell atlas of wt (Wild Type) and ApoE (Apolipoprotein E)-deficient mice defined by single-cell RNA sequencing. *Arterioscler Thromb Vasc Biol*. 2019;39:1055–1071. doi: 10.1161/ATVBAHA.119.312399
42. Kalluri AS, Vellarikkal SK, Edelman ER, Nguyen L, Subramanian A, Ellinor PT, Regev A, Kathiresan S, Gupta RM. Single-cell analysis of the normal mouse aorta reveals functionally distinct endothelial cell populations. *Circulation*. 2019;140:147–163. doi: 10.1161/CIRCULATIONAHA.118.038362
43. van Kuijk K, Kuppe C, Betsholtz C, Vanlandewijck M, Kramann R, Sluimer JC. Heterogeneity and plasticity in healthy and atherosclerotic vasculature explored by single-cell sequencing. *Cardiovasc Res*. 2019;115:1705–1715. doi: 10.1093/cvr/cvz185
44. Wirka RC, Wagh D, Paik DT, Pjanic M, Nguyen T, Miller CL, Kundu R, Nagao M, Coller J, Koyano TK, et al. Atheroprotective roles of smooth muscle cell phenotypic modulation and the TCF21 disease gene as revealed by single-cell analysis. *Nat Med*. 2019;25:1280–1289. doi: 10.1038/s41591-019-0512-5
45. Ubil E, Duan J, Pillai IC, Rosa-Garrido M, Wu Y, Bargiacchi F, Lu Y, Stanbouly S, Huang J, Rojas M, et al. Mesenchymal-endothelial transition contributes to cardiac neovascularization. *Nature*. 2014;514:585–590. doi: 10.1038/nature13839
46. Batlle R, Andrés E, Gonzalez L, Llonch E, Igea A, Gutierrez-Prat N, Berenguer-Llergo A, Nebreda AR. Regulation of tumor angiogenesis and mesenchymal-endothelial transition by p38α through TGF-β and JNK signaling. *Nat Commun*. 2019;10:3071. doi: 10.1038/s41467-019-10946-y
47. Dong W, Li R, Yang H, Lu Y, Zhou L, Sun L, Wang D, Duan J. Mesenchymal-endothelial transition-derived cells as a potential new regulatory target for cardiac hypertrophy. *Sci Rep*. 2020;10:6652. doi: 10.1038/s41598-020-63671-8
48. Meng S, Lv J, Chanda PK, Owusu I, Chen K, Cooke JP. Reservoir of fibroblasts promotes recovery from Limb Ischemia. *Circulation*. 2020;142:1647–1662. doi: 10.1161/CIRCULATIONAHA.120.046872
49. Bentzon JF, Falk E. Circulating smooth muscle progenitor cells in atherosclerosis and plaque rupture: current perspective and methods of analysis. *Vascul Pharmacol*. 2010;52:11–20. doi: 10.1016/j.vph.2009.11.005
50. Bennett MR, Sinha S, Owens GK. Vascular smooth muscle cells in atherosclerosis. *Circ Res*. 2016;118:692–702. doi: 10.1161/CIRCRESAHA.115.306361
51. Haude M, Lee SW, Worthley SG, Silber S, Verheye S, Erbs S, Rosli MA, Botelho R, Meredith I, Sim KH, et al. The REMEDEE trial: a randomized comparison of a combination sirolimus-eluting endothelial progenitor cell capture stent with a paclitaxel-eluting stent. *JACC Cardiovasc Interv*. 2013;6:334–343. doi: 10.1016/j.jcin.2012.10.018
52. Woudstra P, Kalkman DN, Den HP, Menown IB, Erglis A, Suryapranata H, Arkenbout KE, Iñiguez A, Van't Hof AW, Muller P. 1-year results of the remedee registry: clinical outcomes after deployment of the abluminal sirolimus-coated bioengineered (combo) stent in a multicenter, prospective all-comers registry. *JACC Cardiovasc Interv*. 2016;9:1127-1134. doi: 10.1016/j.jcin.2016.02.052
53. Saito S, Krucoff MW, Nakamura S, Mehran R, Maehara A, Al-Khalidi HR, Rowland SM, Tasissa G, Morrell D, Joseph D, et al. Japan-United States of America Harmonized Assessment by Randomized Multicentre Study of OrbusNEich's Combo StEnt (Japan-USA HARMONEE) study: primary results of the pivotal registration study of combined endothelial progenitor cell capture and drug-eluting stent in patients with ischaemic coronary disease and non-ST-elevation acute coronary syndrome. *Eur Heart J*. 2018;39:2460–2468. doi: 10.1093/eurheartj/ehy275
54. Jaguszewski M, Aloysius R, Wang W, Bezerra HG, Hill J, De Winter RJ, Karjalainen PP, Verheye S, Wijns W, Lüscher TF, et al. The REMEDEE-OCT Study: an evaluation of the bioengineered COMBO dual-therapy CD34 antibody-covered sirolimus-eluting coronary stent compared with a cobalt-chromium everolimus-eluting stent in patients with acute coronary syndromes: insights from optical coherence tomography imaging analysis. *JACC Cardiovasc Interv*. 2017;10:489–499. doi: 10.1016/j.jcin.2016.11.040
55. Kipshidze N, Dangas G, Tsapenko M, Moses J, Leon MB, Kutryk M, Serruys P. Role of the endothelium in modulating neointimal formation: vasculoprotective approaches to attenuate restenosis after percutaneous coronary interventions. *J Am Coll Cardiol*. 2004;44:733–739. doi: 10.1016/j.jacc.2004.04.048
56. Sedding DG, Boyle EC, Demandt JAF, Sluimer JC, Dutzmann J, Haverich A, Bauersachs J. Vasa vasorum angiogenesis: key player in the initiation and progression of atherosclerosis and potential target for the treatment of cardiovascular disease. *Front Immunol*. 2018;9:706. doi: 10.3389/fimmu.2018.00706
57. Kusumbe AP, Ramasamy SK, Adams RH. Coupling of angiogenesis and osteogenesis by a specific vessel subtype in bone. *Nature*. 2014;507:323–328. doi: 10.1038/nature13145
58. Patel J, Seppanen EJ, Rodero MP, Wong HY, Donovan P, Neufeld Z, Fisk NM, Francois M, Khosrotehrani K. Functional definition of progenitors versus mature endothelial cells reveals key SoxF-dependent differentiation process. *Circulation*. 2017;135:786–805. doi: 10.1161/CIRCULATIONAHA.116.024754
59. Lukowski SW, Patel J, Andersen SB, Sim SL, Wong HY, Tay J, Winkler I, Powell JE, Khosrotehrani K. Single-cell transcriptional profiling of aortic endothelium identifies a hierarchy from endovascular progenitors to differentiated cells. *Cell Rep*. 2019;27:2748–2758.e3. doi: 10.1016/j.celrep.2019.04.102
60. Kalucka J, de Rooij LPMH, Goveia J, Rohlenova K, Dumas SJ, Meta E, Conchinha NV, Taverna F, Teuwen LA, Veys K, et al. Single-cell transcriptome atlas of murine endothelial cells. *Cell*. 2020;180:764–779.e20. doi: 10.1016/j.cell.2020.01.015
61. Di Bernardini E, Campagnolo P, Margariti A, Zampetaki A, Karamariti E, Hu Y, Xu Q. Endothelial lineage differentiation from induced pluripotent stem cells is regulated by microRNA-21 and transforming growth factor β2 (TGF-β2) pathways. *J Biol Chem*. 2014;289:3383–3393. doi: 10.1074/jbc.M113.495531
62. Piera-Velazquez S, Jimenez SA. Endothelial to mesenchymal transition: role in physiology and in the pathogenesis of human diseases. *Physiol Rev*. 2019;99:1281–1324. doi: 10.1152/physrev.00021.2018
63. Indolfi C, Iaconetti C, Gareri C, Polimeni A, De Rosa S. Non-coding RNAs in vascular remodeling and restenosis. *Vascul Pharmacol*. 2019;114:49–63. doi: 10.1016/j.vph.2018.10.006
64. World_Medical_Association. World medical association declaration of helsinki: ethical principles for medical research involving human subjects. *JAMA*. 2013;310:2191-2194. doi: 10.1001/jama.2013.281053
65. Butler A, Hoffman P, Smibert P, Papalexi E, Satija R. Integrating single-cell transcriptomic data across different conditions, technologies, and species. *Nat Biotechnol*. 2018;36:411–420. doi: 10.1038/nbt.4096
66. Zhou Y, Zhou B, Pache L, Chang M, Khodabakhshi AH, Tanaseichuk O, Benner C, Chanda SK. Metascape provides a biologist-oriented resource

for the analysis of systems-level datasets. *Nat Commun*. 2019;10:1523. doi: 10.1038/s41467-019-09234-6
67. Xie Y, Potter CMF, Le Bras A, Nowak WN, Gu W, Bhaloo SI, Zhang Z, Hu Y, Zhang L, Xu Q. Leptin induces Sca-1+ progenitor cell migration enhancing neointimal lesions in vessel-injury mouse models. *Arterioscler Thromb Vasc Biol*. 2017;37:2114–2127. doi: 10.1161/ATVBAHA.117.309852
68. Deng J, Ni Z, Gu W, Chen Q, Nowak WN, Chen T, Issa Bhaloo S, Zhang Z, Hu Y, Zhou B, et al. Single-cell gene profiling and lineage tracing analyses revealed novel mechanisms of endothelial repair by progenitors. *Cell Mol Life Sci*. 2020;77:5299-5320. doi: 10.1007/s00018-020-03480-4
69. Wang Y, Wang R, Zhang S, Song S, Jiang C, Han G, Wang M, Ajani J, Futreal A, Wang L. iTALK: an R package to characterize and illustrate intercellular communication. *bioRxiv*. Preprint posted online January 4, 2019. doi: 10.1101/507871
70. Cai J, Deng J, Gu W, Ni Z, Liu Y, Kamra Y, Saxena A, Hu Y, Yuan H, Xiao Q, et al. Impact of local alloimmunity and recipient cells in transplant arteriosclerosis. *Circ Res*. 2020;127:974–993. doi: 10.1161/CIRCRESAHA.119.316470
71. Yang F, Chen Q, He S, Yang M, Maguire EM, An W, Afzal TA, Luong LA, Zhang L, Xiao Q. miR-22 is a novel mediator of vascular smooth muscle cell phenotypic modulation and neointima formation. *Circulation*. 2018;137:1824–1841. doi: 10.1161/CIRCULATIONAHA.117.027799
72. Chen T, Karamariti E, Hong X, Deng J, Wu Y, Gu W, Simpson R, Wong MM, Yu B, Hu Y, et al. DKK3 (Dikkopf-3) transdifferentiates fibroblasts into functional endothelial cells-brief report. *Arterioscler Thromb Vasc Biol*. 2019;39:765–773. doi: 10.1161/ATVBAHA.118.311919